

# Separation and Detection of 2,3-Dihydroxybenzoic Acid

Stephanie E. Hooper

Thesis submitted to the Faculty of the Virginia Polytechnic Institute and State University  
in partial fulfillment of the requirements for the degree of

Master of Science  
in  
Chemistry

Dr. Mark R. Anderson, Chair

Dr. Gary L. Long

Dr. T. Daniel Crawford

August 17, 2004

Blacksburg, Virginia

Keywords: capillary electrophoresis, electrochemical and UV/Vis detection,  
oxidative stress

Copyright 2004, Stephanie E. Hooper

## **Separation and Detection of 2,3-Dihydroxybenzoic Acid**

By

Stephanie E. Hooper

(ABSTRACT)

In Parkinson's disease, severe damage to nigrostriatal neurons causes a depletion of the neurotransmitter dopamine (DA). Oxidative stress on the brain is thought to contribute to neuron cell death and to the onset of Parkinson's disease. Reactive oxygen radicals produced during oxidative stress have been implicated as an initiator of neuron destruction. Glutamate, an excitatory neurotransmitter, can initiate OH radical formation when present in excess. Oxidative stress on the brain caused by glutamate overflow may be monitored by trapping the OH radicals with salicylic acid to produce 2,3-dihydroxybenzoic acid (2,3-DHBA). Determination of this product is initially performed using capillary zone electrophoresis (CZE) coupled with UV detection to establish optimum separation conditions. These conditions were applied for rapid, efficient, and sensitive determination of 2,3-DHBA by CZE coupled with electrochemical detection. Quick and sensitive detection of 2,3-DHBA is essential in monitoring OH radical generation and identifying its role in Parkinson's disease.

## **Acknowledgements**

I would like to thank my family for their undying support in all that I have done. They have been there every step of the way, and I only hope I can return the sentiment ten fold. I love you all very much.

Thanks to Dr. Mark R. Anderson, whose brilliance, guidance, and patience were more than I could have ever hoped for in an advisor. I would like to thank my fellow group members: Alice Harper, who I've shared so much more with than just an office, Huimin Li, and especially David Roach, whose aid in my research was crucial and appreciated more than he knows.

I would like to thank past and present members of my committee: Dr. Brian Tissue, Dr. T. Daniel Crawford, and Dr. Gary Long.

A very special thanks is reserved for Sheila Gradwell, Mary Tam, and Joshua Uzarski who have kept me sane throughout this process and mean more to me than they will ever know.

I would also like to thank God for anything and everything that has come to be in my life.

## Table of Contents

Acknowledgements.....	iii
Table of Contents.....	iv
Table of Figures.....	vi
List of Tables.....	viii
Chapter 1: Separation and Detection of 2,3-Dihydroxybenzoic Acid.....	1
1.1 Introduction.....	1
1.2 Principles of Capillary Electrophoresis.....	4
1.3 Detection Schemes in Capillary Zone Electrophoresis.....	8
1.3.1 Laser-Induced Fluorescence.....	8
1.3.2 Ultraviolet Detection.....	9
1.3.3 Electrochemical Detection.....	11
1.4 Thesis Statement.....	13
Chapter 2: Experimental Details.....	14
2.1 Chemicals and Solutions Used.....	14
2.2 Capillary Treatment and Conditioning for UV analysis.....	14
2.3 Capillary Treatment and Conditioning for Electrochemical Analysis.....	15
2.4 Instrumental Setup and Parameters for CZE/UV Analysis.....	15
2.5 Method for Preparation of Carbon Fiber Microelectrodes.....	17
2.6 Testing of Carbon Fiber Microelectrodes.....	17
2.7 Instrumental Setup and Parameters for Electrochemical Analysis.....	18
Chapter 3: Capillary Zone Electrophoresis Coupled with on-column UV Detection.....	20
3.1 Introduction.....	20
3.2 Results and Discussion.....	20
3.2.1 Wavelength Selection.....	20
3.2.2 Separation.....	21
3.2.3 UV Detection Limits.....	24
3.3 Polycationic Capillary Modification.....	28
3.3.1 Poly( <i>diallyldimethylammonium chloride</i> ) ( <i>PDADMAC</i> ) as a cationic coating.....	28
3.3.2 Capillary Coating Procedure.....	29
3.4 PDADMAC Modification Results and Discussion.....	30
3.4.1 Separation.....	30
3.4.1.1 Effect of PDADMAC concentration on flow rate.....	31
3.4.1.2 Effect of PDADMAC concentration on electrophoretic mobility ( $\mu_e$ ).....	32
3.4.1.3 Effect of PDADMAC concentration on elution time of 2,3-DHBA.....	33
3.4.1.4 Effect of PDADMAC concentration on Efficiency ( <i>N</i> ).....	34
3.4.1.5 Effect of Inner Diameter size on 2,3-DHBA response.....	35
3.5 Conclusions.....	36
Chapter 4: Capillary Zone Electrophoresis Coupled with End-column Electrochemical Detection.....	39
4.1 Introduction.....	39
4.2 Results and Discussion.....	39
4.2.1 Oxidation Potential Selection.....	39
4.2.2 Separation Results with Direct End-Column Amperometric Detection.....	40
4.2.3 Direct End-Column Amperometry Detection Limits.....	43

4.2.4 <i>Separation Results with End-Column Pulsed Amperometric Detection</i> .....	44
4.2.5 <i>Pulsed Amperometric Limits of Detection</i> .....	48
4.3 Conclusions.....	50
Chapter 5: Summary and Future Work.....	52
5.1 Summary .....	52
5.2 Future Work .....	52
References.....	54
Vita.....	58

## Table of Figures

Figure 1. Molecular structure of Dopamine.....	1
Figure 2. Molecular structure of Glutamate.....	2
Figure 3. Hydroxyl radical trapping reaction.....	3
Figure 4. Typical Capillary Electrophoresis setup.....	5
Figure 5. Electroosmotic flow in normal/positive polarity mode.....	6
Figure 6. Flow Profiles: EOF vs. Pressure.....	7
Figure 7. Instrumental Setup and Design for CZE/UV Analysis.....	16
Figure 8. 3 mM DA in 0.1 M KCl with carbon microelectrode.....	18
Figure 9. Electrochemical cell setup for CZE/ED.....	19
Figure 10. UV Spectrum of MO, DA, and 2,3-DHBA to determine optimal wavelength selection for each compound.....	21
Figure 11. Electropherogram of 2.5 pmol DA, 0.5% MO, and 2.5 pmol 2,3-DHBA using a 50 $\mu$ m ID capillary with 15 kV applied voltage.....	22
Figure 12. Electropherograms of 1.25 pmol 2,3-DHBA with applied voltages of 10, 15, and 20 kV using a 75 $\mu$ m ID capillary.....	23
Figure 13. Calibration curve for 2,3-DHBA in pH 7, 50 mM phosphate buffer using a 50 cm length 25 $\mu$ m ID capillary with a 15 kV applied separation voltage.....	25
Figure 14. Calibration curve for 2,3-DHBA in pH 7, 50 mM phosphate buffer using a 50 cm length 50 $\mu$ m ID capillary with a 15 kV applied separation voltage.....	25
Figure 15. Calibration curve for DA in pH 7, 50 mM phosphate buffer using a 50 cm length 25 $\mu$ m ID capillary with a 15 kV applied separation voltage.....	26
Figure 16. Calibration curve for DA in pH 7, 50 mM phosphate buffer using a 50 cm length 50 $\mu$ m ID capillary with a 15 kV applied separation voltage.....	27
Figure 17. Reversed EOF in Normal/Positive Polarity Mode.....	28
Figure 18. Structure of PDADMAC.....	29
Figure 19. Electropherogram of 2.5 pmol 2,3-DHBA and 0.5% MO on a 50 cm length 50 $\mu$ m ID capillary modified with 1 mM PDADMAC. Separation voltage of 15 kV..	30
Figure 20. Electropherogram of 2.5 pmol 2,3-DHBA on 10mM, 5mM, and 1mM PDADMAC 50 $\mu$ m ID Coated Capillaries with an applied voltage of 15 kV.....	33
Figure 21. Electropherograms of 2.5 pmol 2,3-DHBA using 25, 50, 75 $\mu$ m ID capillaries with an applied voltage of 15 kV.....	36
Figure 22. Cyclic voltammograms of 3 mM DA and 2,3-DHBA in 50mM Phosphate Buffer (pH 7) at 100 mV/s.....	40
Figure 23. Electropherogram of 5.5 fmol DA and 5.5 fmol catechol using a 60 cm length 20 $\mu$ m ID capillary with 15kV applied voltage and applied potential of 650 mV....	41
Figure 24. Electropherogram of 5.5 fmol DA and 5.5 fmol 2,3-DHBA using a 60 cm length 20 $\mu$ m ID capillary with 15kV applied voltage and applied potential of 650 mV.....	42
Figure 25. Calibration curve for DA using a 60 cm length 20 $\mu$ m ID capillary with applied potential of 650mV.....	43
Figure 26. Pulsed electropherogram of 1.67 fmol DA, 4-AR, and Catechol using a 60 cm length 20 $\mu$ m ID capillary with separation voltage of 15 kV.....	46
Figure 27. Pulsed electropherogram of 2.78 fmol 2,3-DHBA and DOPAC using a 60 cm length 20 $\mu$ m ID capillary with separation voltage of 15 kV.....	47

Figure 28. Calibration curve for DA using a 60 cm length 20 $\mu\text{m}$ ID capillary with a pulsed potential of 650mV.....	48
Figure 29. Calibration curve for 2,3-DHBA using a 60 cm length 20 $\mu\text{m}$ ID capillary with a pulsed potential of 650 mV.....	49

## List of Tables

Table 3.1. Flow rate values for 50 $\mu\text{m}$ ID capillaries uncoated and modified with 0.5, 1, 5, and 10 mM PDADMAC.....	31
Table 3.2. Electrophoretic mobility values for 50 $\mu\text{m}$ ID capillaries uncoated and modified with 0.5, 1, 5, and 10 mM PDADMAC.....	32
Table 3.3. Efficiency of 2.5 pmol 2,3-DHBA and 0.5% MO at varying concentrations of PDADMAC on a 50 $\mu\text{m}$ ID capillary with an applied voltage of 15 kV.....	35



## Chapter 1: Separation and Detection of 2,3-Dihydroxybenzoic Acid

### 1.1 Introduction

Parkinson's Disease (PD) is a neurologically degenerative disease whose pathogenesis is not wholly understood.<sup>1</sup> PD affects about one percent of the population

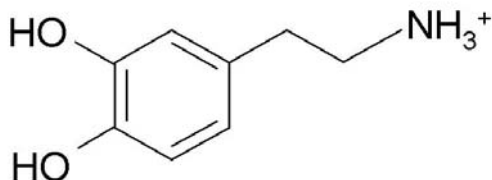


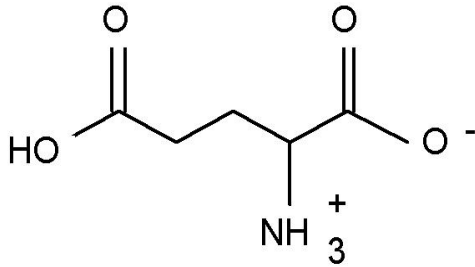
**Figure 1. Molecular Structure of Dopamine**

over the age of 60. Distinctive symptoms of this disease include rigidity, tremors, unstable posture, and more prevalently bradykinesia or slow movement.<sup>1</sup> The onset of these symptoms occurs when the nigrostriatal portion of the brain experiences a deficiency in the neurotransmitter dopamine (DA).<sup>2</sup>

Dopamine is the neurotransmitter responsible for locomotion and cognition.<sup>3</sup> Loss of these functions is detrimental to an individual's quality of life.

Factors such as genetics, environmental toxin exposure, and head trauma have been associated with the onset of PD, although no single cause has yet been implicated.<sup>4</sup> One hypothesis is that oxidative stress in the brain could contribute to neuron cell death due to their susceptibility to attack from free radicals.<sup>4</sup> Oxidative stress is the generation of highly reactive oxygen radicals during cell metabolism caused by defective electron transport in the mitochondria and neurotoxin exposure. This can lead to oxidative damage in proteins, DNA, and cells.<sup>4</sup> The use of N-methyl D-aspartate (NMDA) antagonists is one treatment that has shown promise at lowering neurotoxic effects due to oxidative stress.<sup>5</sup>

The NMDA receptor is one of three receptors for glutamate, the most prevalent excitatory neurotransmitter in the brain.<sup>6</sup>



Glutamate

**Figure 2. Molecular Structure of Glutamate**

When glutamate is released into the synapse, the junction between two neurons, it can bind with the NMDA receptor. This aids in regulation of calcium influx into neuron cells by preventing Ca<sup>2+</sup> from reaching lethal

levels. When glutamate is present in excess, this initiates the production of

reactive oxygen species (ROS) such as the hydroxyl radical. This could lead to oxidative stress conditions in the brain, leading to neuronal cell death.<sup>6</sup>

The hydroxyl radical is viewed as the most toxic and reactive of all ROS.<sup>8</sup> In vivo determination of this radical has proven difficult in the past.<sup>9</sup> The OH radical is highly reactive, so it has a short half-life existing in trace-level concentrations. Electron spin resonance (ESR) could be used for direct determination of OH•, but there are limitations to this method such as the need for spin traps and high expense.<sup>10</sup> The most common method for monitoring oxidative stress is by trapping hydroxyl radicals with salicylic acid as shown in Figure 3.<sup>7</sup> The reaction product here is 2,3-dihydroxybenzoic acid (2,3-DHBA), an analyte with a long lifetime that is easily measured either by electrochemistry or spectroscopy.



requiring minimal sample volumes ( $\mu\text{L}$  to  $\text{nL}$ )<sup>15</sup>, so it becomes advantageous over previous analytical methods for determination of 2,3-DHBA as a marker for oxidative stress.

## **1.2 Principles of Capillary Electrophoresis**

CE was first introduced as an analytical separation technique by Jorgenson and Lukacs in 1981.<sup>14</sup> Electrophoresis occurs when a high enough dc electric field is applied to a buffer causing charged species to migrate at various rates through buffer. Jorgenson showed that if high voltages were applied to buffer filled capillaries of small inner diameters, efficient, quick separation of ionic species could also be achieved. High separation voltages will result in rapid migration times, and using smaller inner diameter capillaries allow for more even dissipation of Joule heat, generated by current passage through the buffer medium.<sup>14-15</sup>

A typical CE setup is shown in Figure 4. A buffer filled fused silica capillary usually 40-100 cm in length extends between two buffer reservoirs. Capillary inner diameter sizes typically fall in the range of 10 to 100  $\mu\text{m}$ . A high voltage power supply applies separation voltages between 0 and 30 kV. A platinum electrode is immersed in both the buffer solutions as a high voltage is applied along the length of the capillary. If a positive voltage is applied to the high voltage electrode, the ground end electrode becomes cathodic by default. A fixed detector is placed towards the ground end of the capillary.

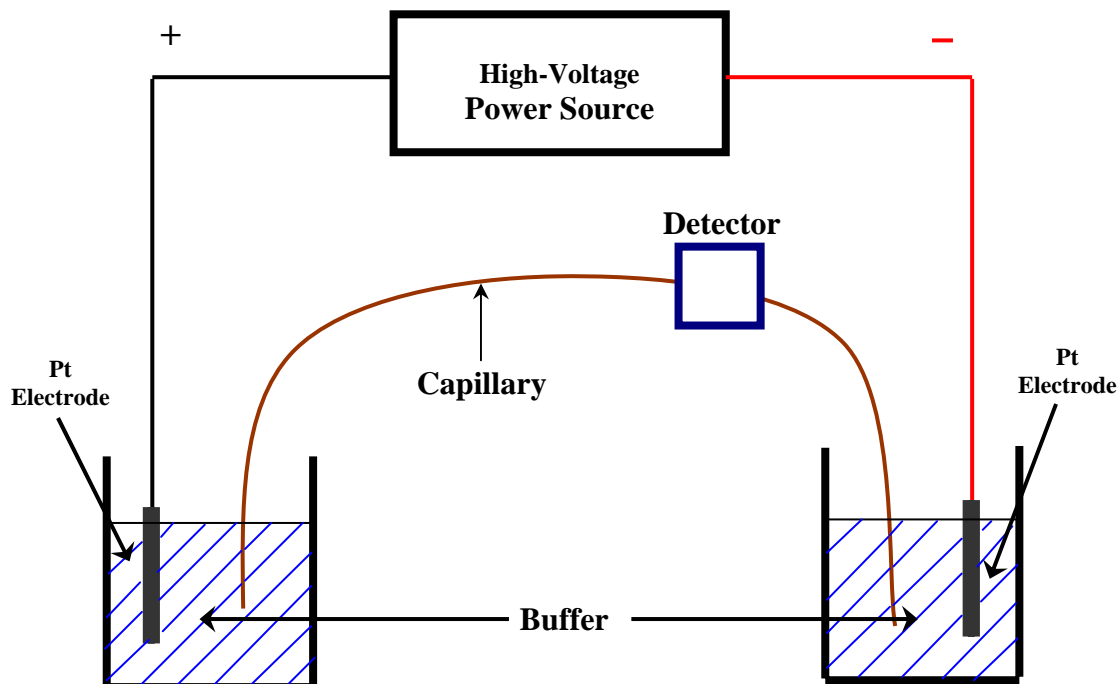


**Figure 4. Typical Capillary Electrophoresis setup**

The driving force to ion migration in CE is due to what is called electroosmotic flow (EOF). Electroosmosis creates a bulk flow of buffer solution through the capillary to the detector.<sup>19</sup> EOF is caused by the formation of an electric double layer (EDL) at the silica/solvent interface as illustrated in Figure 5. Above pH values of 3, the capillary wall silanol groups are dissociated, creating a fixed negative charge along the capillary wall. This negative charge attracts positive ions in the buffer solution, effectively creating an EDL at the capillary wall. These positive ions in the EDL are attracted to the negative ground electrode end of the capillary, and migrate toward that end of the capillary under the influence of the electric field. The large concentration of cations moving along the

inner capillary wall essentially drags along the solvent as well, creating the EOF.

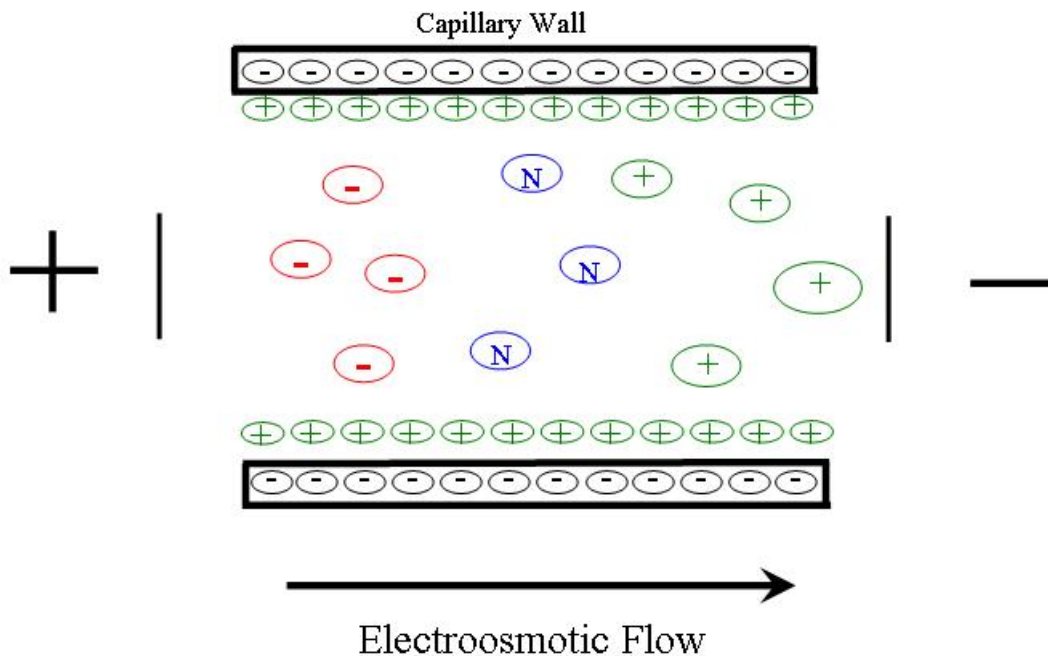


**Figure 5. Electroosmotic flow in normal/positive polarity mode**

EOF is dependent on the buffer pH, as pH affects the charge of the capillary wall silanol groups.<sup>19</sup> At pH 7, EOF is strong enough to sweep cations, neutral species, and anionic species through the capillary. This would consequently be the elution order of the resulting electropherogram if a positive separation voltage were applied. EOF effectively moves all ionic species through the capillary, yet analytes still migrate at different rates based on their charge and size.<sup>19</sup> EOF allows CE to be an elution method, making it a versatile separation technique.

One advantage EOF offers within CE is reduced peak broadening as compared to HPLC.<sup>18</sup> Electroosmotic-driven flow produces a flat flow profile of solution through the capillary, whereas pressure driven flow in HPLC creates a parabolic flow profile as illustrated in Figure 6.<sup>18</sup> The flat profile produces uniform distribution of solution along the width of the capillary.<sup>51</sup> The parabolic profile is due to frictional forces along the capillary wall, generating different flow velocities along the capillary diameter.<sup>51</sup>

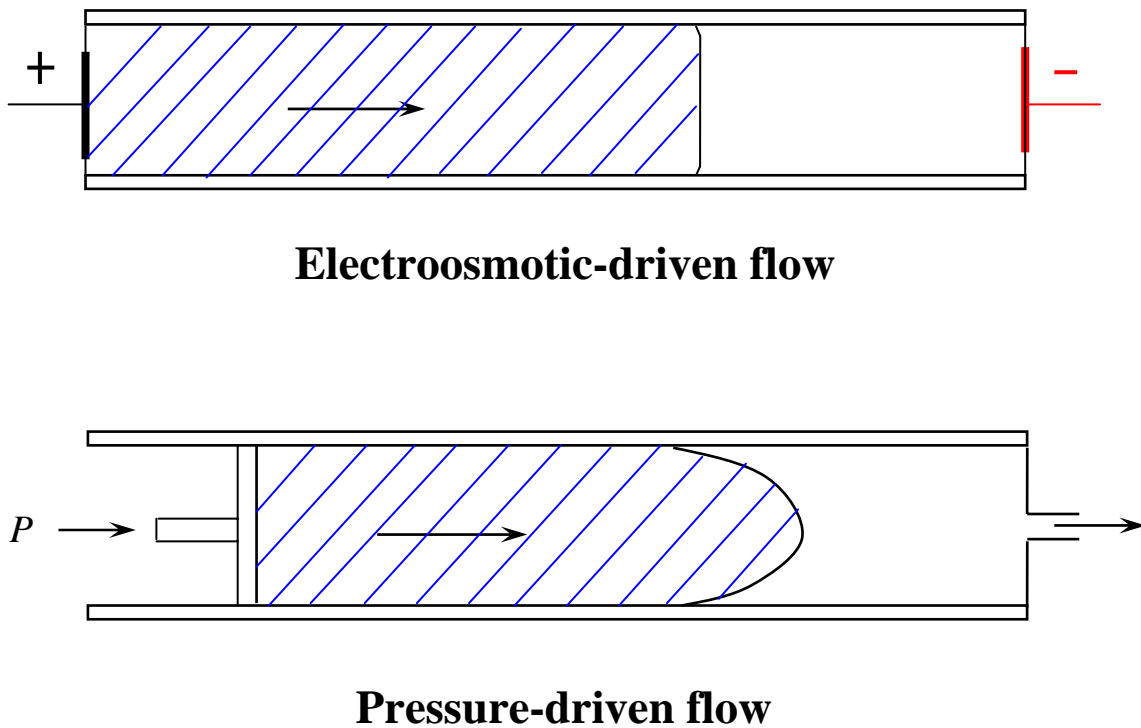


**Figure 6. Flow Profiles: EOF vs. Pressure**

Within CE, there are several modes to perform ionic separations. The three main methods are capillary isotachopheresis, capillary isoelectric focusing, and capillary zone electrophoresis (CZE).<sup>17</sup> CZE is the most common type of CE used in analytical

separations<sup>17</sup> and is utilized in our research. CZE occurs when ions separate into distinct bands or zones with buffer between each zone. The buffer composition remains constant throughout the separation in CZE.

CZE is a highly efficient separation method which can be determined by the number of theoretical plates. Separation efficiency is directly proportional to the applied voltage, and it is independent of the capillary length unlike in HPLC.<sup>16</sup> Typical theoretical plate values for CZE are 50,000-200,000 as compared to standard plate values of 5,000 to 20,000 for HPLC. Theoretical plates as high as one million have been reported for CZE.<sup>20</sup>

CZE is a useful elution method for investigating 2,3-DHBA primarily because minimal sample size is needed for future in vivo applications. CZE also demonstrates versatility with the various detection schemes it can be coupled with.

### **1.3 Detection Schemes in Capillary Zone Electrophoresis**

CZE has been coupled with several different detection methods since its emergence as an analytical technique. The most common detection modes are laser-induced fluorescence (LIF), ultraviolet (UV), and electrochemical detection (ED).<sup>21</sup>

#### ***1.3.1 Laser-Induced Fluorescence***

When Jorgenson and Lukacs first performed zone electrophoresis of amino acids in capillaries, their method of detection was an on-column homemade fluorescence detector.<sup>14</sup> The development of LIF as a detection method for CZE has since progressed greatly. CZE/LIF has a large neurological application due to its high sensitivity and low sampling volumes that are needed for high temporal resolution in microdialysis for



example.<sup>52-53</sup> CZE/LIF has been coupled with microdialysis for in-line determination of the amino acid neurotransmitters aspartate and glutamate<sup>53</sup>, the catecholamines dopamine and noradrenaline<sup>52</sup>, and ascorbic acid<sup>54</sup>. Although LIF provides extremely sensitive detection limits, derivatization of many samples is required before analysis adding complexity and cost to the system. Ultraviolet detection offers a simpler, more versatile detection scheme for CZE.

### ***1.3.2 Ultraviolet Detection***

The use of on-column UV detection with CE was first reported by Tsuda and coworkers in 1983 for the separation of pyridinium salts, metal ions, and sulphonic acids.<sup>22</sup> They supplied few details of the UV detection parameters. Walbroehl and Jorgenson developed an on-column UV detector in 1984 used in the separation of isoquinoline and lysozyme.<sup>23</sup> Theirs was a good reproducible system as they developed a way to secure the capillary through the detector. Interference filters were used to select the desired wavelength for detection. A detector window was made by removing a small section of the polyimide coating on the fused silica capillary to allow the transmission of UV light. Fused silica is transparent to approximately 190 nm.<sup>23</sup> This on-column UV detector is the basis for most optical detectors used today in conjunction with CZE.

On-column UV detection is the most prominent detection scheme used in CZE.<sup>15</sup> It is versatile as many compounds absorb in the UV region. Frequently wavelengths between 200 and 220 nm are utilized due to strong absorbance of many analytes in this region. No derivatization or modification of samples is usually necessary, so UV detection is generally more applicable than LIF. Unfortunately, CZE/UV lacks the

sensitivity of LIF, as the small inner diameter size of the capillary limits the UV light path length. Extending the path length, reducing the noise from the detector, or optimal wavelength selection are ways to improve poor sensitivity.<sup>15</sup> The use of a diode array spectrometer allows for multichannel monitoring of several wavelengths, so the optimum or most discriminating wavelength for each analyte can be applied. This gives CZE/UV adequate selectivity while its sensitivity is modest compared with other detection schemes.

CZE/UV has been utilized for the environmental analysis of EDTA<sup>55</sup> and phenolic compounds<sup>56</sup>. CZE/UV has hardly been employed for the analyte of interest, 2,3-DHBA. Tjornelund separated several hydroxy and dihydroxybenzoic acids in a non-aqueous media using CZE/UV.<sup>24</sup> The running buffer was a methanol/acetonitrile mixture, while detection was carried out at 214 nm.<sup>24</sup> Coolen investigated 2,3 and 2,5-DHBA as products of hydroxylation with salicylic acid using CZE/UV.<sup>25</sup> Detection was performed at 200 nm, with a Tris buffer at pH 2.78 as the background electrolyte.<sup>25</sup> Limits of detection are reported in following experimental results chapters.

CZE/UV offers a simple, useful detection scheme for many compounds, yet it lacks the sensitivity necessary for monitoring trace levels found in the brain. CZE/LIF possesses this sensitivity, but sample derivatization is often required which adds complexity, time, and cost to the analytical system. CZE coupled with electrochemical detection (CZE/ED) offers the high sensitivity of LIF, while remaining a simple, cost-effective technique. The small capillaries necessary for CZE/ED are also complimentary to the small sample size limitation encountered in hydroxyl trapping research.

### ***1.3.3 Electrochemical Detection***

Electrochemical detection has proven to be a viable, sensitive method for measurements of many biological compounds, including neurotransmitters.<sup>27</sup> Many neurotransmitters are catecholamines or derivatives of catechol that can be easily measured by electrochemical oxidation.<sup>28</sup>

End-column electrochemical detection coupled with CZE was first introduced by Wallingford and Ewing in 1987 for the analysis of catechol and catecholamines.<sup>26</sup> This was done using a carbon fiber microelectrode as the working electrode placed at the end of a 75  $\mu\text{m}$  inner diameter capillary.

Carbon fiber microelectrodes as working electrodes are regularly used for in vivo electrochemical determination of neurological compounds.<sup>30</sup> Microelectrodes are also useful for CZE/ED systems because their dimensions correspond with the small inner diameter sizes of capillaries.<sup>29</sup>

Wallingford and Ewing employed amperometric detection of catecholamines to achieve detection limits in the pmol range.<sup>26</sup> Direct amperometric detection is commonly utilized in many analyses.<sup>29</sup> This means the applied potential is held constant, while the corresponding current response is measured as the analytical signal.

However, in CE coupled with amperometric detection interference from the separation voltage with the applied working electrode potential can occur.<sup>30</sup> This can be eliminated by decoupling the large separation voltage from the voltage applied to the working electrode. Decoupling can be accomplished through using fractures or porous joints at the end of the capillary, very small inner diameter capillaries, and low conductivity buffers.<sup>30</sup>

Wallingford and Ewing initially used a porous glass joint at the cathodic end of the capillary for decoupling.<sup>26</sup> They soon improved the separation efficiency and detection limits of catechols and neurotransmitters (fmol-amol range) by using smaller ID capillaries of sizes 26  $\mu\text{m}$  and 12.5  $\mu\text{m}$  without the need for a porous glass joint.<sup>31-32</sup> Sloss and Ewing further enhanced decoupling with the use of 2  $\mu\text{m}$  ID size capillaries for detection of catechol.<sup>57</sup> Using small ID capillaries evolved as the simplest, most efficient method for decoupling as long as the distance between the electrode and the end of the capillary is minimized.<sup>58</sup>

CZE/ED has since been further developed for the analysis of neurotransmitters and catecholamines. There have been advancements in optimum separation conditions, electrochemical cells, decouplers, and applications to microdialysis studies.<sup>33-37</sup> CZE coupled with amperometric detection has evolved as a sensitive, efficient separation/detection scheme for catechol-like compounds.

CZE/ED can further be enhanced by using pulsed amperometric detection (PAD). PAD improves signal to noise of the system, thus giving rise to more sensitive current response. PAD steps between different set potentials, measuring the current at each potential. The background current measured at the initial potential can be subtracted from the current generated at the detection potential, thus enhancing signal to noise.

O'Shea and Lunte reported the first separation and detection by CE/PAD in 1993 for the analysis of carbohydrates.<sup>59</sup> The working electrode was a 50 $\mu\text{m}$  gold wire.<sup>59</sup> LaCourse and Owens further developed CE/PAD to analyze amino acids, thiocompounds, and disulfides also utilizing a gold wire working electrode.<sup>60-61</sup> All

CE/PAD studies reported have used metals such as gold, platinum, or copper as the working electrode.

Only one study on PAD using carbon fiber microelectrodes has been reported thus far. Here, PAD was coupled with HPLC for the determination of furosemide.<sup>62</sup> No reports utilizing CE coupled with PAD using carbon fiber microelectrodes have been found. Thus, our determination of 2,3-DHBA utilizing CZE/PAD is a novel and sensitive approach towards monitoring oxidative stress.

#### **1.4 Thesis Statement**

Using capillary zone electrophoresis coupled with ultraviolet detection, the optimum conditions for the rapid, efficient, and selective determination of 2,3-dihydroxybenzoic acid are determined. These conditions are then applied to coupling CZE with amperometric and pulsed amperometric detection for more sensitive detection of 2,3-DHBA. Improved separation and detection of 2,3-dihydroxybenzoic acid as a bona fide marker for oxidative stress may eventually lead to better understanding of hydroxyl radical generation and their toxic, harmful neurological effects.

## **Chapter 2: Experimental Details**

### **2.1 Chemicals and Solutions Used**

Solutions of known concentration were prepared from the following compounds of interest: 2,3-dihydroxybenzoic acid (2,3-DHBA, 99% from Aldrich), 3-hydroxytyramine hydrochloride also known as dopamine (DA, 98% from Aldrich), mesityl oxide (MO, 90% from Aldrich), catechol (99% from Aldrich), 3,4-dihydroxyphenylacetic acid (DOPAC, 98% from Aldrich), and 4-aminoresorcinol hydrochloride (97% from Aldrich). All solutions for ultraviolet detection analysis were prepared in 50 mM phosphate buffer (pH 7) made from sodium phosphate monobasic and sodium phosphate dibasic heptahydrate (Fisher) diluted with nanopure water. All solutions for electrochemical analysis were prepared in 50 mM KCl/ 10 mM phosphate buffer (pH 7) made from potassium chloride (Fisher), sodium phosphate monobasic and sodium phosphate dibasic heptahydrate (Fisher) diluted with nanopure water. Capillaries were modified with PDADMAC (20% in water from Aldrich).

### **2.2 Capillary Treatment and Conditioning for UV analysis**

Fused silica capillaries (Polymicro Technologies) with 360  $\mu\text{m}$  outer diameter and varying inner diameters of 75  $\mu\text{m}$ , 50  $\mu\text{m}$ , and 25  $\mu\text{m}$  were cut to an approximate length of 50 cm by placing both ends under tension, cleaving at a 30 degree angle with a ceramic capillary cutting tool, and pulling apart for a clean break. This allows for unrestricted, even flow through the capillary. A detector window at a length of 37 cm was prepared by burning and removing a 1 cm portion of the outer polyimide coating. All capillaries were conditioned with 0.1 M NaOH for 30 minutes and 50 mM Phosphate

Buffer (pH 7) for 30 minutes. Solutions of NaOH and Phosphate Buffer are pushed through the capillary at low pressures using nitrogen gas. A pH close to 7 is optimal for mimicking physiological pH (7.4) and conditions for current and future research applications.

### **2.3 Capillary Treatment and Conditioning for Electrochemical Analysis**

Fused silica capillaries with 360  $\mu\text{m}$  outer diameter and 20  $\mu\text{m}$  inner diameter were cut to approximate lengths of 60 cm by the cleaving procedure discussed above in section 2.2. 20  $\mu\text{m}$  ID capillaries were used because they are small enough to minimize the interference from the separation voltage with the working electrode potential as discussed in the introduction chapter. Capillaries were conditioned by pushing the following solutions through by low pressure using nitrogen gas. Capillaries were treated with 0.1 M NaOH for 30 minutes and 50 mM KCl/ 10mM Phosphate Buffer (pH 7) for 30 minutes. The KCl/Phosphate Buffer served as the running buffer for all CE/ED experiments. For separations involving anionic species, capillaries were modified by flushing the capillary with 0.1 M NaOH for 30 minutes, then a 1 mM PDADMAC solution for an hour, and finally rinsed with the running buffer. A concentration of 1 mM PDADMAC was selected for this modification because it resulted in the most favorable separation conditions for 2,3-DHBA at pH 7 as described in chapter 3.

### **2.4 Instrumental Setup and Parameters for CZE/UV Analysis**

Capillary zone electrophoresis was performed with the aforementioned capillaries utilizing a Spellman CZE1000R high voltage power supply. The high voltage end of the

power supply is placed in an isolated plexiglass box where injections are carried out in order to ensure the safety of the analyst. When the box is opened, a safety switch automatically turns off the power supply while injection is made. Once the lid is closed, power returns to its original setting and separation continues. The detection is carried out at the ground end of the capillary. Ultraviolet detection is performed with an Ocean Optics USB2000 diode array spectrometer. The capillary is secured at its detection window using a P-729 Peek Cross providing a reproducible optical path length and fairly stable baseline. A separation voltage of 15 kV was applied along the length of the capillary.

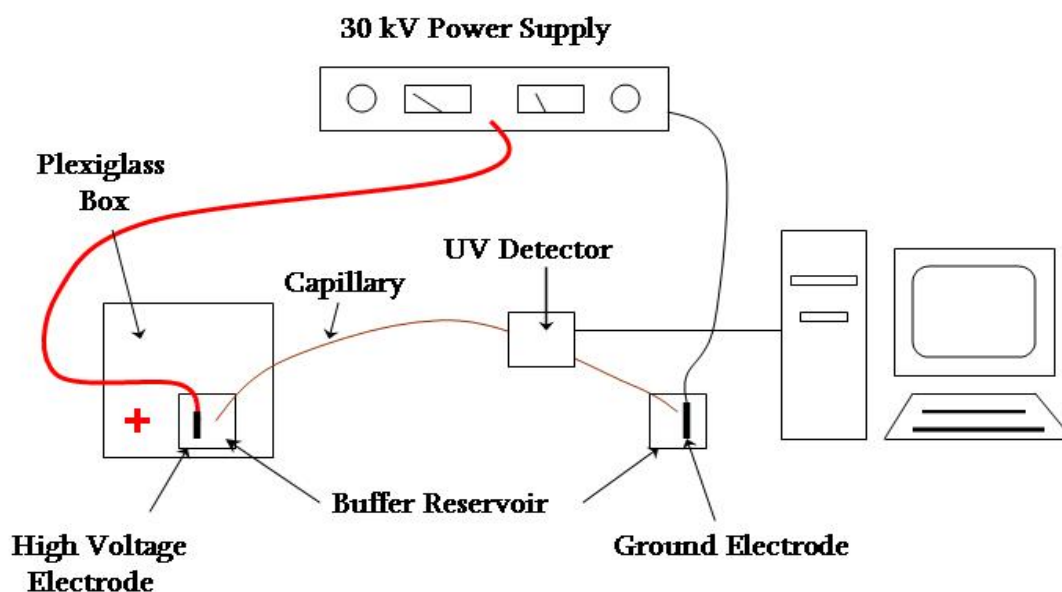


**Figure 7. Instrumental Setup and Design for CZE/UV Analysis**



## **2.5 Method for Preparation of Carbon Fiber Microelectrodes**

Single carbon fibers (Thornel, type P-55) are aspirated into glass capillaries (Kimax, 1.5-1.8 x 100 mm). The capillary ends are pulled to fine points using a capillary puller. The carbon fiber is then sealed into the tapered end with epoxy (Shell Epon Resin) and rinsed with acetone to remove excess epoxy from the exposed fiber. The exposed fiber ends are cut under a microscope so that a length of the fiber as close to 10 $\mu$ m as possible protrudes from the seal with the glass. The microelectrodes are left overnight at room temperature for the epoxy to harden. They are then cured in an oven at 100°C for 2 hours and 150°C for an additional 2 hours, and then allowed to cool to room temperature.

## **2.6 Testing of Carbon Fiber Microelectrodes**

To determine if an electrode is viable for detection and analysis, it must first be tested using cyclic voltammetry (CV). The microelectrode is filled with an acetate solution (4 M Na<sup>+</sup>CH<sub>3</sub>COO<sup>-</sup>/0.15 M NaCl) which acts as a capacitive junction between the carbon fiber and a metal wire that is inserted into the open end of the capillary. A test solution of 3mM DA is made in 0.1 M KCl. The carbon microelectrode serves as the working electrode, a platinum wire acts as the auxiliary electrode, and a Ag/AgCl electrode is used as the reference electrode. The potential is typically cycled from 0 V to 1 V back to 0 V at a scan rate of 100 mV/s. An acceptable electrode will produce a sigmoidal-shaped curve indicative of steady mass transport behavior with a current

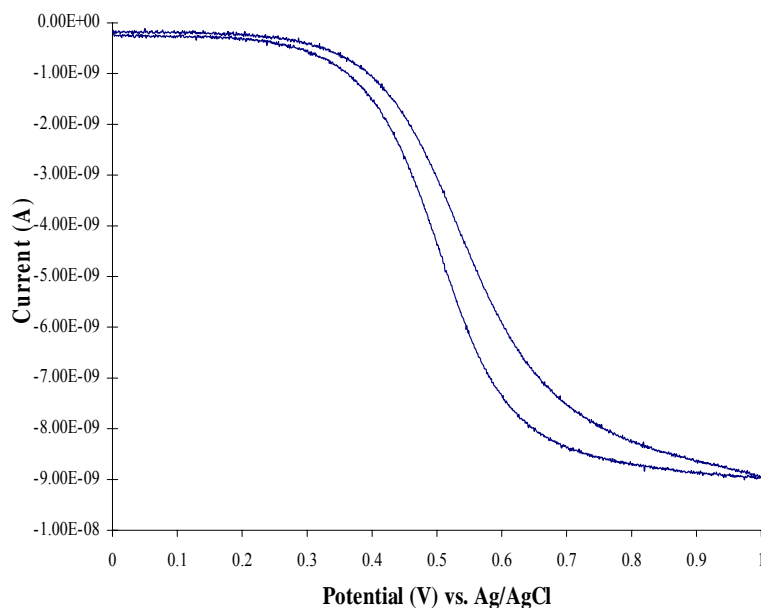


**Figure 8. 3 mM DA in 0.1M KCl  
with carbon microelectrode**

response typically in the nanoamp range.<sup>48</sup> Figure 8 is an example of a cyclic voltammogram for the oxidation of DA.

## 2.7 Instrumental Setup and Parameters for Electrochemical Analysis

CZE was performed with the conditioned capillaries described in section 2.3. The experimental setup is the same as described in section 2.4 except for the detection carried out. Electrochemical detection is performed at the ground end of the capillary with the microelectrode aligned with the open end of the capillary. The potentiostat used in this system is from Princeton Applied Research, Model 273. Solution flows into the electrochemical cell shown below (Figure 9) and past the carbon fiber microelectrode where analytes get oxidized, and the current response is measured by the potentiostat. Alignment of the microelectrode with the end of the capillary was

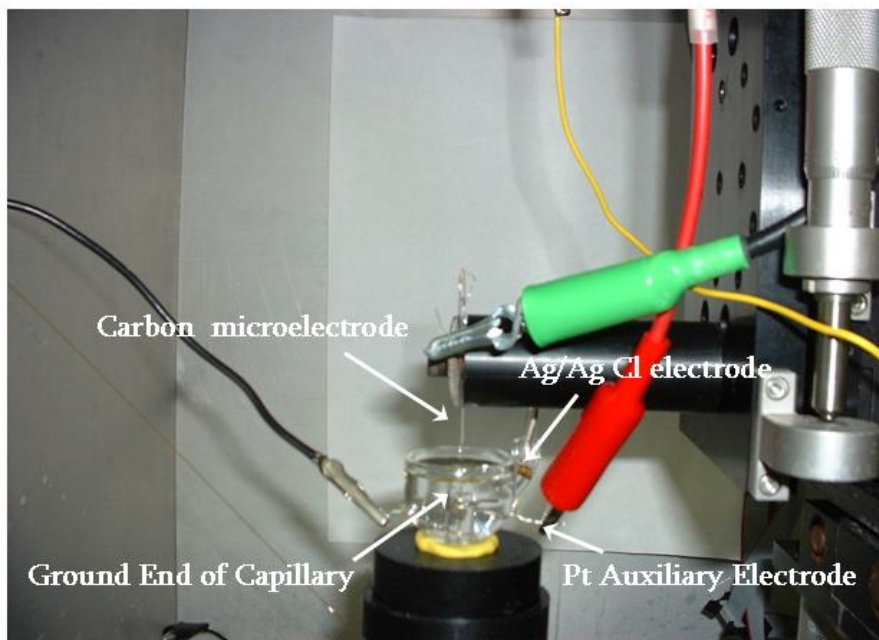


**Figure 9. Electrochemical cell setup for CZE/ED**

achieved with the aid of a stereomicroscope and XYZ positioner. For all amperometric experiments, a potential of 650 mV vs. Ag/AgCl was applied to the carbon fiber working electrode. A separation voltage of 15 kV was applied along the length of the capillary.

## Chapter 3: Capillary Zone Electrophoresis Coupled with on-column UV Detection

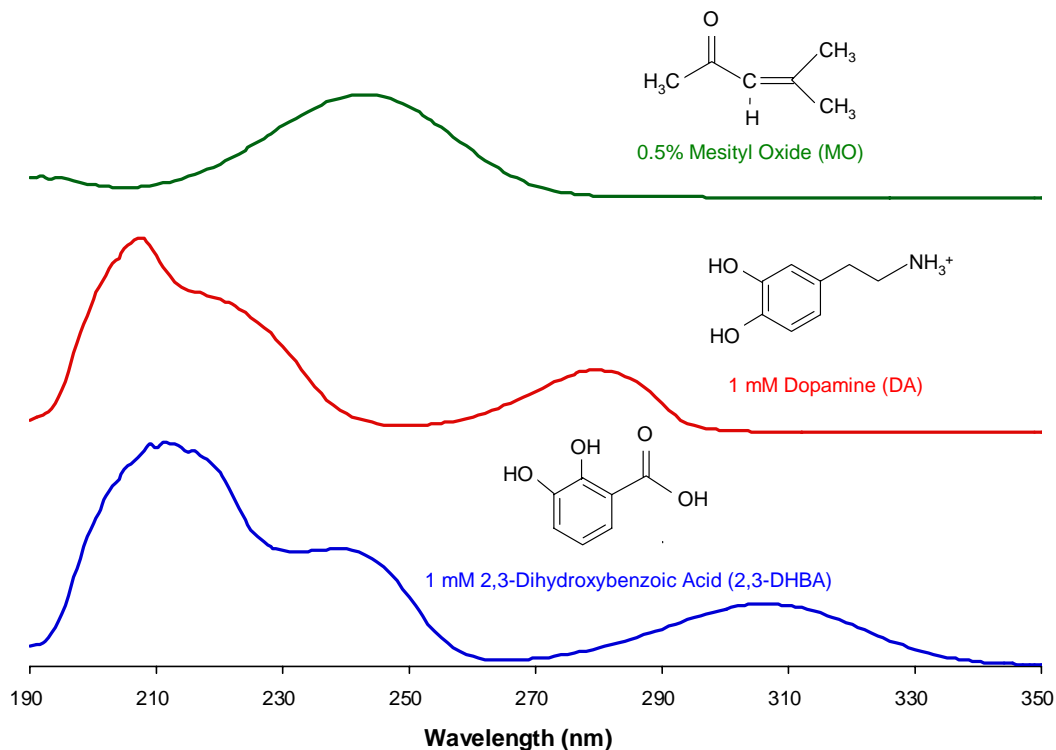
### 3.1 Introduction

CZE coupled with UV detection is a useful, versatile technique to determine if 2,3-DHBA can be separated and detected in solution. While UV detection lacks sensitivity, CZE/UV was helpful in establishing the optimal conditions and parameters for the determination of 2,3-DHBA. These conditions were then applied for simpler, more sensitive detection of 2,3-DHBA electrochemically discussed in chapter 4.

### 3.2 Results and Discussion

#### 3.2.1 Wavelength Selection

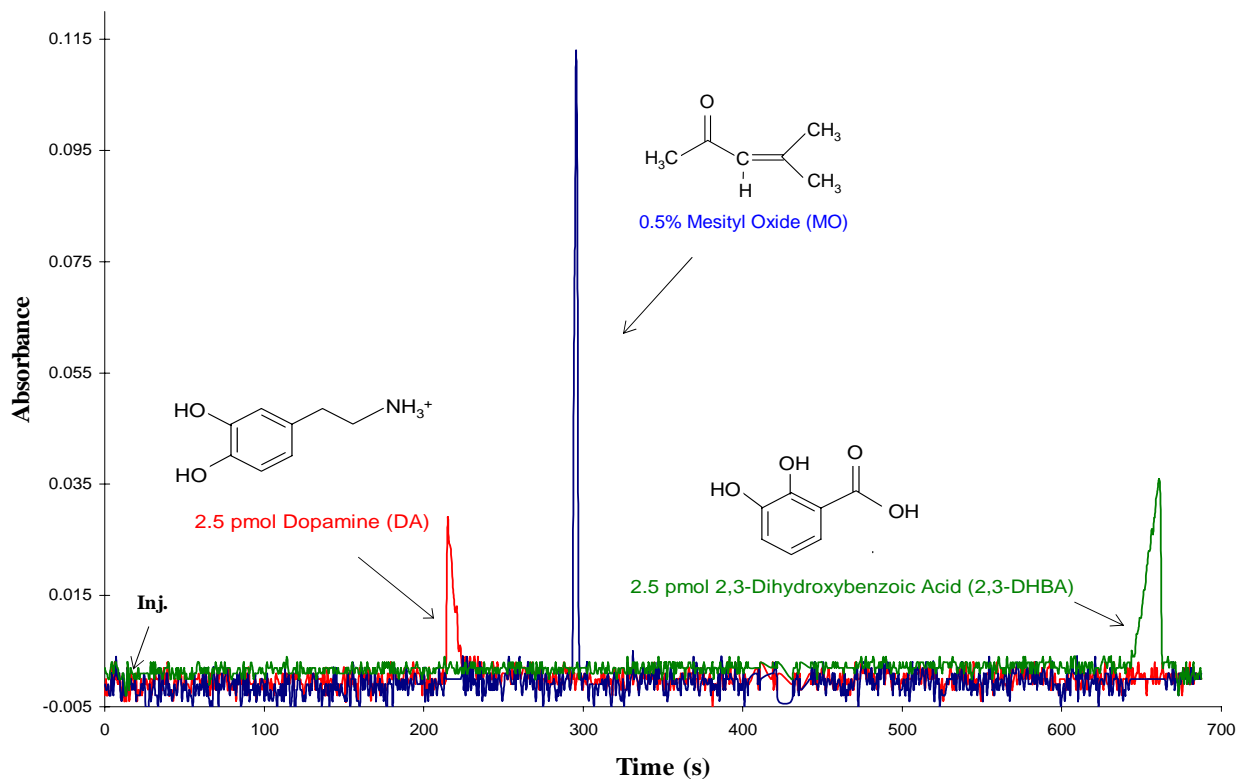
Optimal wavelength selection allows for increased selectivity for each analyte and multichannel monitoring of each compound during the separation. Figure 10 shows the UV/Vis spectrum of mesityl oxide (MO), dopamine (DA), and 2,3-dihydroxybenzoic acid (2,3-DHBA). The selected wavelengths are 240 nm for MO, 280 nm for DA, and 310 nm for 2,3-DHBA. These three compounds were also modeled at these three wavelengths using CaChe to obtain their HOMO and LUMO orbitals. This provided information that suggested the most likely transition for each selected wavelength is  $\pi$  to  $\pi^*$ . Each experimental UV spectra for MO, DA, and 2,3-DHBA are consistent with theoretical UV transitions determined using CaChe as well.



**Figure 10. UV Spectrum of MO, DA, and 2,3-DHBA to determine optimal wavelength selection for each compound.**

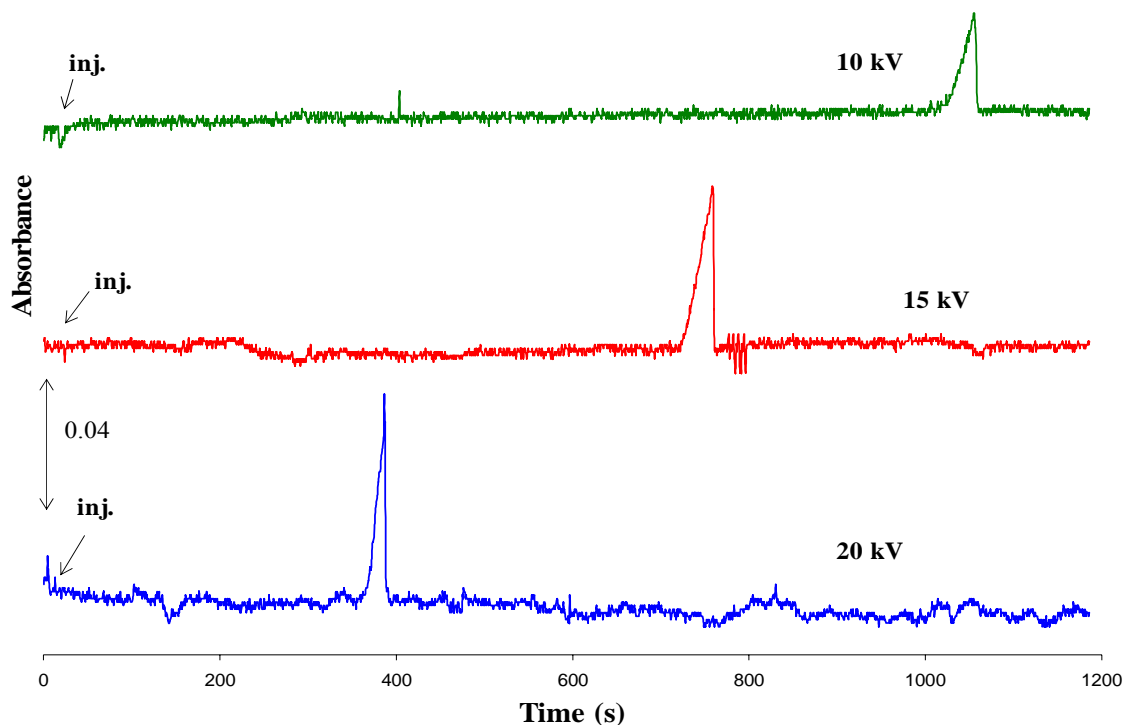
### 3.2.2 Separation

Figure 11 shows the separation electropherogram for DA, MO, and 2,3-DHBA using a 50  $\mu\text{m}$  ID capillary. The order of elution is based on the direction of the electroosmotic flow (EOF) which is toward the cathodic/detector end of the capillary in this case. Since the buffer pH is 7, DA will elute first (pKa of 8.60), then MO which serves as a neutral marker and moves at the same rate of the EOF, and finally 2,3-DHBA (pKa of 2.97).



**Figure 11. Electropherogram of 2.5 pmol DA, 0.5% MO, and 2.5 pmol 2,3-DHBA using a 50  $\mu\text{m}$  ID capillary with 15 kV applied voltage.**

Elution times appear to be approximately four minutes for DA, five minutes for MO, and eleven minutes for 2,3-DHBA. These retention times are fairly similar when using 25  $\mu\text{m}$  and 75  $\mu\text{m}$  ID capillaries. A study was done to investigate the effect of the applied separation voltage on resolution and elution times, namely for the analyte of interest, 2,3-DHBA using a 75  $\mu\text{m}$  ID capillary.



**Figure 12. Electropherograms of 1.25 pmol 2,3-DHBA with applied voltages of 10, 15, and 20 kV using a 75  $\mu\text{m}$  ID capillary.**

At higher applied voltages, 2,3-DHBA elutes much more quickly and its peak appears more sharply defined. So as the separation voltage is increased, analytes are swept through the capillary faster. However, the baseline for the 20 kV electropherogram has more noise and is not as stable as that for 10 or 15 kV separations. This could be problematic at lower concentrations where signal to noise becomes an important analytical consideration. Also, at high voltages (20 kV and above) one may encounter the problem of Joule heating, which is generated from the passage of current through the running buffer.<sup>39</sup> Joule heating can result in unequal thermal dispersion throughout the

capillary disrupting the flow of ions, essentially ending the separation.<sup>15</sup> Thus 15 kV was selected as a suitable value for an applied voltage.

### ***3.2.3 UV Detection Limits***

A study was performed to determine the limits of detection (LOD) for both DA and 2,3-DHBA using capillaries of varying inner diameter. The following figures are the calibration curves and resulting LODs for each analyte. LOD values are determined by adding the mean background absorbance signal to three times the standard deviation of the mean background signal. This sum was divided by the slope of the calibration curve. This procedure allows determination of the LOD in mM which is converted to moles by assuming a detection volume (of a cylinder) in  $\text{cm}^3$  for a 50  $\mu\text{m}$  and 25  $\mu\text{m}$  ID capillary. The volume of a cylinder is given as  $\pi r^2 h$  where  $r$  is the radius of the ID of the capillary (25 or 12.5  $\mu\text{m}$ ) and  $h$  is the height of the light source slit which is 25  $\mu\text{m}$ . Once the moles of analyte are determined, the mass can be calculated by simply multiplying by the molecular weight of DA (189.64 g/mol) or 2,3-DHBA (154.12 g/mol). Limits of linearity (LOL) could not be determined for ultraviolet detection because no concentrations above 100 mM were evaluated where the calibration curve could begin to deviate from linearity.



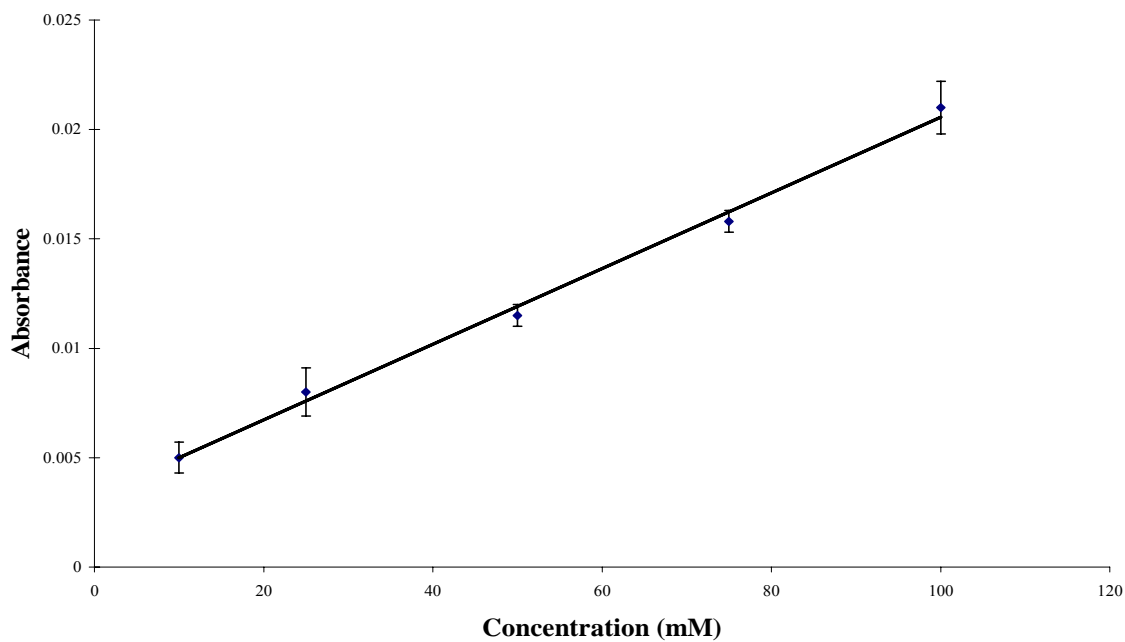


**Figure 13. Calibration Curve for 2,3-DHBA in pH 7, 50 mM phosphate buffer using a 50 cm length 25  $\mu\text{m}$  ID capillary with a 15 kV applied separation voltage.**

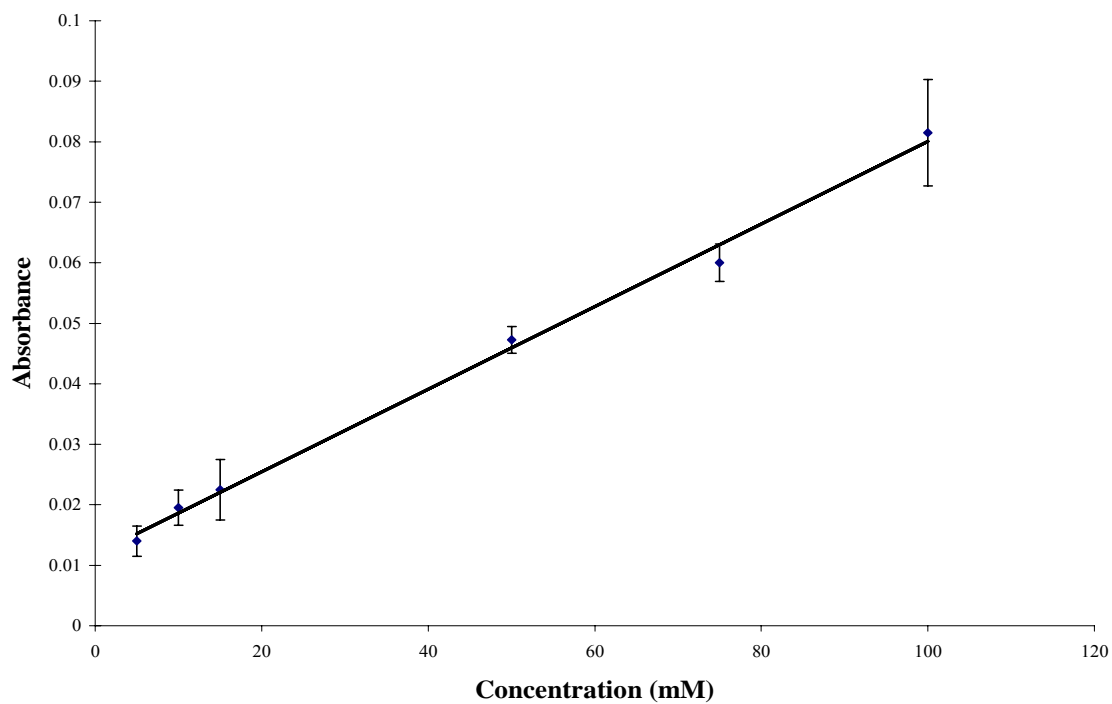


**Figure 14. Calibration Curve for 2,3-DHBA in pH 7, 50 mM phosphate buffer using a 50 cm length 50  $\mu\text{m}$  ID capillary with a 15 kV applied separation voltage.**

The UV detection limit for 2,3-DHBA with a 25  $\mu\text{m}$  ID capillary is 0.29 pmol or 44 pg and is 0.76 pmol or 120 pg for a 50  $\mu\text{m}$  ID capillary. The only study found to have analyzed 2,3-DHBA using CZE/UV by Coolen, et. al reported a LOD value of  $2.0 \times 10^{-7}$  M.<sup>25</sup> This study utilized a 75  $\mu\text{m}$  ID capillary with a Tris buffer of pH 2.78, a distant value from physiological pH. Their detection wavelength was 200 nm, as most compounds strongly absorb in this region.<sup>25</sup> Detection in our system occurs at 310 nm which is a more discriminating wavelength against DA and MO.

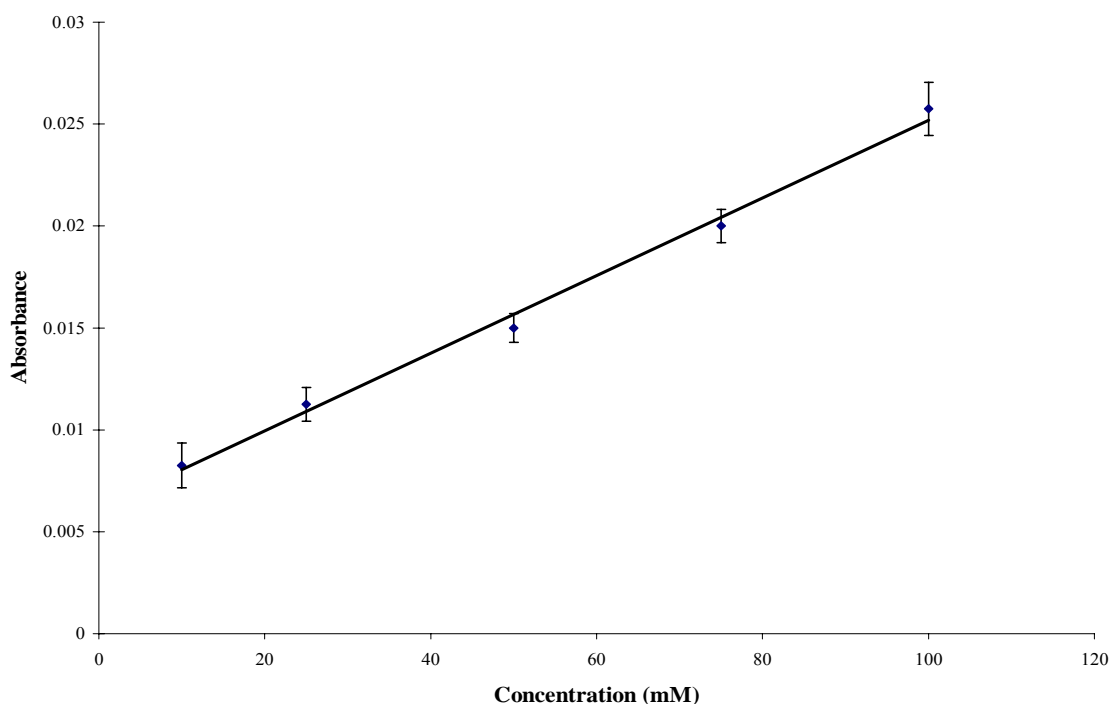


**Figure 15. Calibration curve for DA in pH 7, 50 mM phosphate buffer using a 50 cm length 25  $\mu\text{m}$  ID capillary with a separation voltage of 15 kV.**

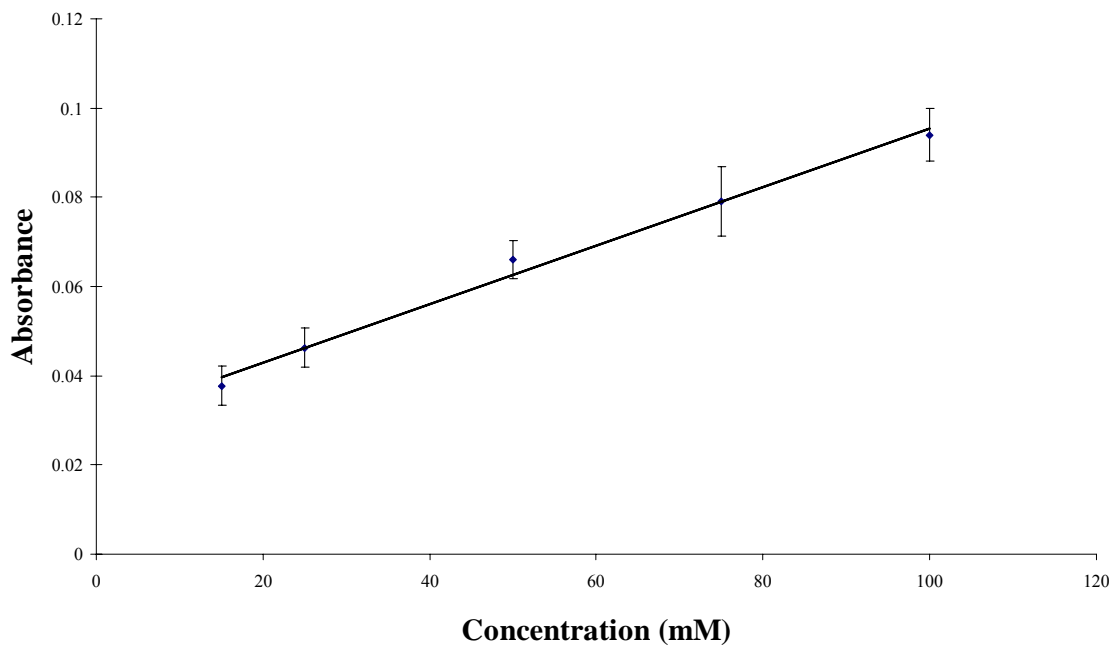


**Figure 16. Calibration Curve for DA in pH 7, 50 mM phosphate buffer using a 50 cm length 50  $\mu$ m ID capillary with a separation voltage of 15 kV.**

The detection limit for DA using a 50  $\mu$ m ID capillary is 0.46 pmol or 88  $\mu$ g and is 0.49 pmol or 93  $\mu$ g with a 25  $\mu$ m ID capillary. Recent LOD values reported for DA with CZE/UV are 3-14 fmol.<sup>40-41</sup> These studies were done using a 50 $\mu$ m ID capillary with a borate/acetate buffer of pH 10. The detection wavelength was 214 nm where compounds absorb more strongly.<sup>40-41</sup> Comparison of our DA LOD values to these recent literature values is not practical as separation conditions and detection parameters differ.

### 3.3 Polycationic Capillary Modification

#### 3.3.1 Poly(*diallyldimethylammonium chloride*) (PDADMAC) as a cationic coating

One approach to separate and detect the analyte of interest, 2,3-DHBA, more quickly and efficiently is to reverse the direction of electroosmotic flow (EOF). Reversing the EOF using negative polarity leads to improved separation and faster elution times for anions such as 2,3-DHBA.<sup>42</sup> Several methods exist to reverse the EOF that include the use of surfactants, chemical bonding or covalent coating of the inner capillary wall, and polycationic/anionic electrolytes.<sup>43</sup> Polycations act as a positively charged stationary phase through ionic interactions with the Si surface effectively reversing the EOF as illustrated below in Figure 17.<sup>42</sup>

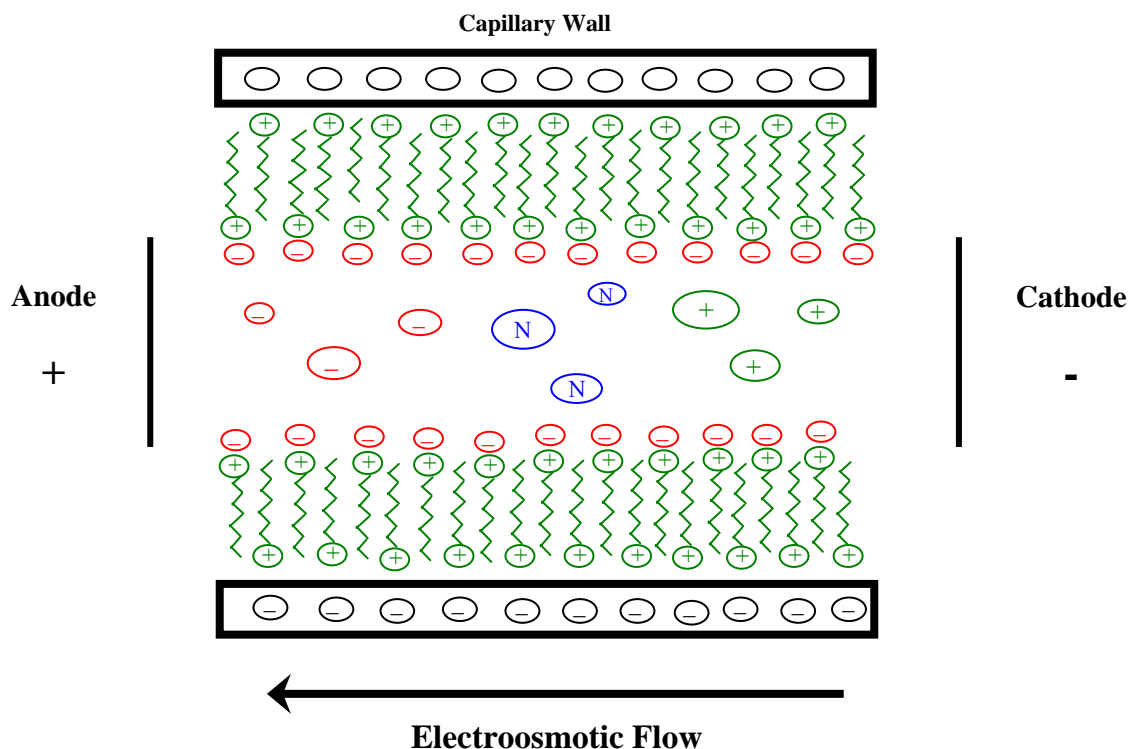


**Figure 17. Reversed EOF in Normal/Positive Polarity Mode**

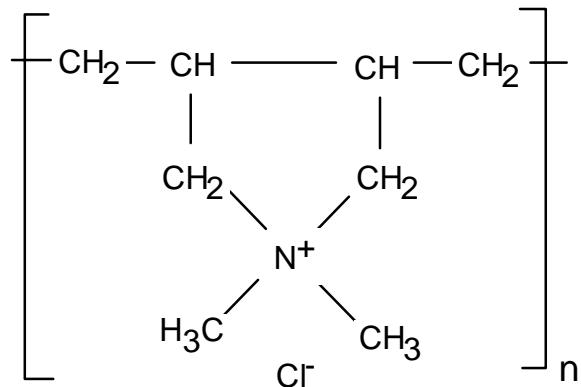


**Figure 18. Structure of PDADMAC**

Poly(ethyleneimine) (PEI), poly(diallyldimethylammonium chloride) (PDADMAC), and (diethylamino) ethyldextran (DEAE dextran) are common cationic polymers used to modify the inside walls of a capillary.<sup>43</sup>

PDADMAC possesses quaternary ammonium groups so it is likely to remain

positively charged over a wide pH range independent of the background electrolyte.<sup>44</sup>

PDADMAC is a very stable cationic polymer, and it has a relatively easy coating procedure.<sup>45</sup> This enables PDADMAC to be an optimal polycation for the reversal of EOF.

### ***3.3.2 Capillary Coating Procedure***

Capillaries were cut and prepared as the previously described method in section 2.2, while the conditioning procedure differed slightly. All conditioning solutions were pushed through the capillary by pressure with nitrogen gas. All capillaries were flushed with 0.1 M NaOH for 30 minutes, then PDADMAC solutions of varying concentration for one hour to allow ample time for electrostatic assembly, and finally rinsed with 50 mM Phosphate Buffer (pH 7). All PDADMAC solutions were prepared in the background electrolyte (Phosphate Buffer).

### 3.4 PDADMAC Modification Results and Discussion

#### 3.4.1 Separation

Electrostatic assembly of PDADMAC to the fused silica capillary to reverse the EOF should allow for faster and better separation of the anionic analyte of interest, 2,3-DHBA. The following electropherogram suggests this is true as the elution time of 2,3-DHBA decreases from 11 minutes on an unmodified capillary to 3 minutes on a capillary modified with PDADMAC.

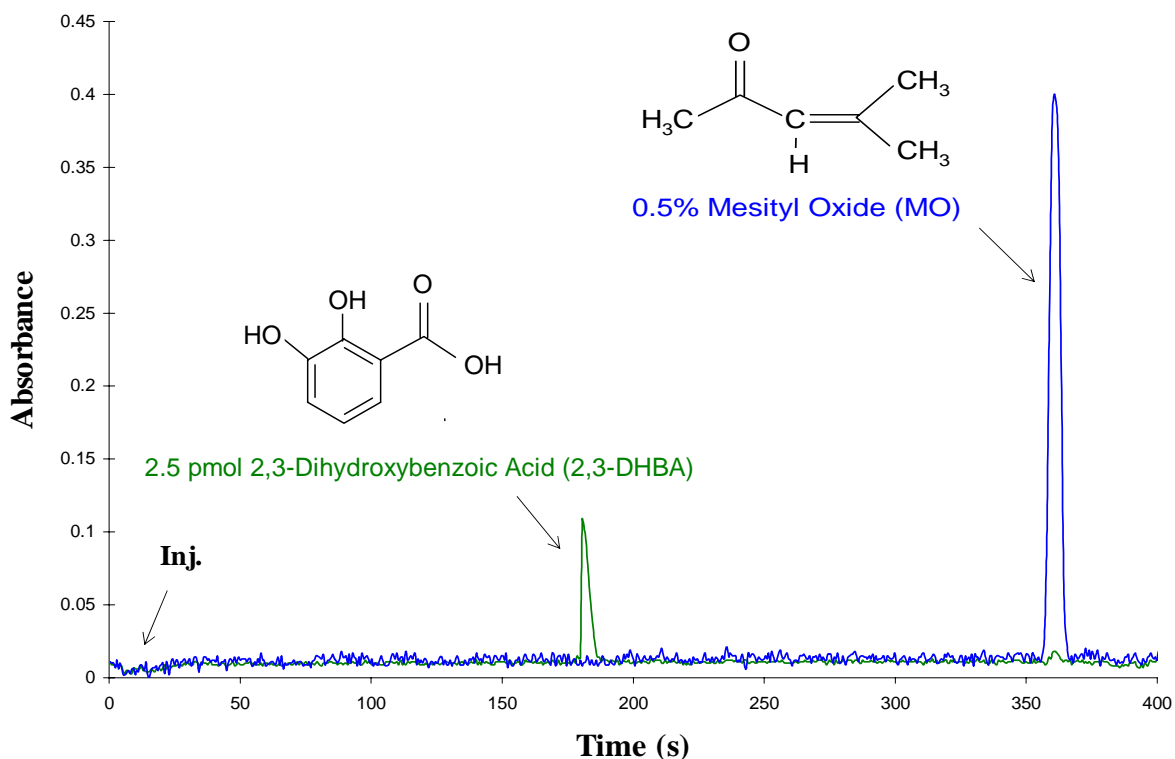


**Figure 19. Electropherogram of 2.5 pmol 2,3-DHBA and 0.5% MO on a 50 cm length 50  $\mu$ m ID capillary modified with 1 mM PDADMAC. Separation voltage of 15 kV.**

The effect of PDADMAC concentration on the flow rate, electrophoretic mobility, efficiency, and elution time of 2,3-DHBA and MO was determined. MO was

used as a reference for the rate of the EOF since neutral species elute at the same rate as the EOF.

### 3.4.1.1 Effect of PDADMAC concentration on flow rate

The flow rate was calculated through a series of conversions involving the capillary inner diameter, length to detector window, and elution time. First, the volume of solution to the detector window was determined assuming the volume of a cylinder ( $\pi r^2 h$ ) where  $r$  is the ID of the capillary and  $h$  is the capillary length to the detector window. This volume is divided by the elution time of the analyte to determine the flow rate.

**Table 3.1. Flow rate values for 50  $\mu$ m ID capillaries uncoated and modified with 0.5, 1, 5, and 10 mM PDADMAC.**

<b>Coated 50 <math>\mu</math>m ID capillary (50 cm length)</b>	<b>EOF/MO (0.5%) Flow Rate (<math>\mu</math>L/min.)</b>	<b>2,3-DHBA (2.5 pmol) Flow Rate (<math>\mu</math>L/min.)</b>
<b>Uncoated</b>	<b>0.158</b>	<b>0.068</b>
<b>10 mM PDADMAC</b>	<b>0.069</b>	<b>0.162</b>
<b>5 mM PDADMAC</b>	<b>0.082</b>	<b>0.185</b>
<b>1 mM PDADMAC</b>	<b>0.122</b>	<b>0.261</b>
<b>0.5 mM PDADMAC</b>	<b>0.125</b>	<b>0.271</b>

The flow rate for the analyte of interest, 2,3-DHBA, dramatically increased when flowing through a PDADMAC modified capillary, and the EOF was less restricted at lower PDADMAC concentrations. This indicates that the anionic species, 2,3-DHBA, is

moving much more quickly through a capillary coated with a lower concentration of PDADMAC.

### 3.4.1.2 Effect of PDADMAC concentration on electrophoretic mobility ( $\mu_e$ )

Electrophoretic mobility ( $\mu_e$ ) of an ion is based on its mass to charge ratio, so how quickly it migrates is dependent on its interaction with other ions and the capillary wall.<sup>42</sup> The electrophoretic mobility ( $\mu_e$ ) of a specific analyte can be defined as the difference of the apparent mobility ( $\mu_{app}$ ) and the electroosmotic flow ( $\mu_{eof}$ ) of the system. The apparent mobility of an ion ( $\mu_{app}$ ) can also be determined by the following formula:

**Equation 3.1.**  $\mu_{app} = (L_d L_t) / (t_m V)$

$L_d$  is the length of the capillary to the detector,  $L_t$  is the total length of the capillary,  $V$  is the applied voltage, and  $t_m$  is the elution time of the analyte.<sup>42</sup>

**Table 3.2. Electrophoretic mobility values for 50  $\mu$ m ID capillaries uncoated and modified with 0.5, 1, 5, and 10 mM PDADMAC.**

Coated 50 $\mu$ m ID capillary (50 cm length)	EOF/MO (0.5%) $\mu_e$ ( $\text{cm}^2/\text{Vs}$ )	2,3-DHBA (2.5 pmol) $\mu_e$ ( $\text{cm}^2/\text{Vs}$ )
Uncoated	$4.18 \times 10^{-4}$	$2.26 \times 10^{-4}$
10 mM PDADMAC	$1.92 \times 10^{-4}$	$2.66 \times 10^{-4}$
5 mM PDADMAC	$2.32 \times 10^{-4}$	$2.74 \times 10^{-4}$
1 mM PDADMAC	$3.46 \times 10^{-4}$	$3.94 \times 10^{-4}$
0.5 mM PDADMAC	$3.51 \times 10^{-4}$	$4.16 \times 10^{-4}$



The data in table 3.2 indicates that 2,3-DHBA has less interaction with ions or the capillary wall at lower concentrations of PDADMAC, thus it migrates more rapidly through the capillary. A similar trend exists for the EOF as well, supporting the flow rates determined earlier.

### 3.4.1.3 Effect of PDADMAC concentration on elution time of 2,3-DHBA

Elution times were monitored at three different concentrations of PDADMAC (1, 5, and 10 mM) to see if faster, better separation occurred with lower concentrations as suggested by the flow rate and electrophoretic mobility data.

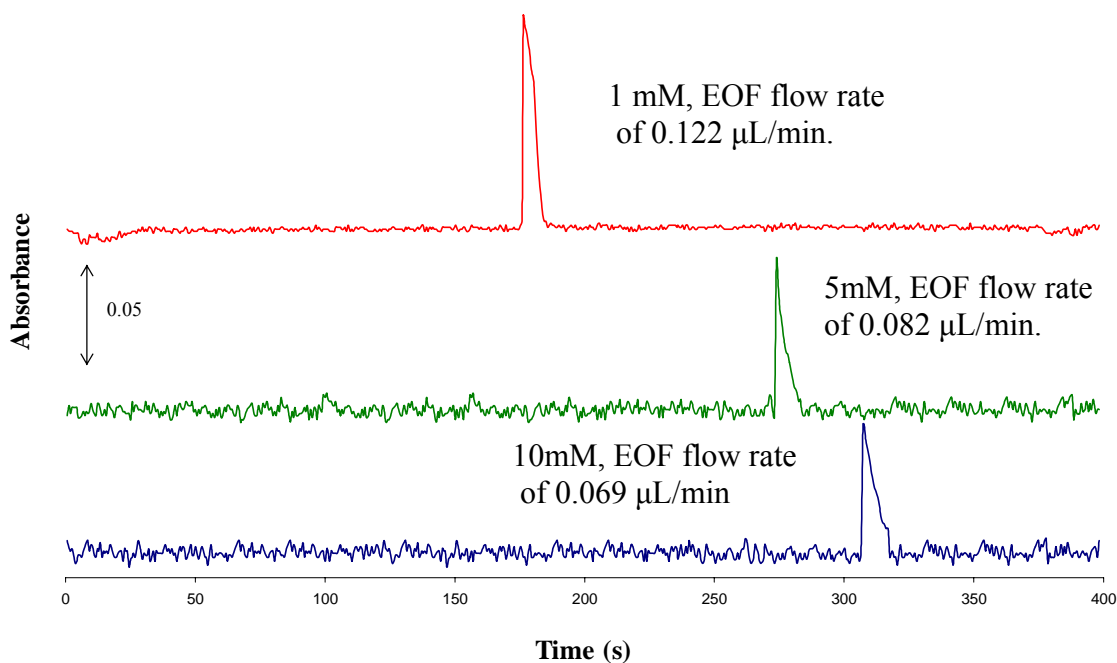


**Figure 20. Electropherogram of 2.5 pmol 2,3-DHBA on 10mM, 5mM, and 1mM PDADMAC 50 $\mu\text{m}$  ID Coated Capillaries with an applied voltage of 15 kV.**

2,3-DHBA has the fastest elution time through the capillary modified with 1 mM PDADMAC. Its peak is better defined on the 1mM coated capillary as compared with the 5 and 10 mM modified capillaries.

#### ***3.4.1.4 Effect of PDADMAC concentration on Efficiency (N)***

Separation efficiency is defined by the number of theoretical plates calculated for a specific peak. Greater numbers of theoretical plates result in narrower peaks, and better separation efficiency. Efficiency for a CZE separation can be calculated by the following equation.<sup>14</sup>

***Equation 3.2.***  $N = (\mu_e E) / 2 D$

Here, D is the diffusion coefficient of the analyte,  $\mu_e$  is the electrophoretic mobility of the ion, and E is the electric field.<sup>14</sup> 2,3-DHBA values for  $\mu_e$  are listed in Table 3.2. D is assumed to be  $0.5 \times 10^{-6} \text{ cm}^2/\text{s}$ , as this value could not be found in the literature for 2,3-DHBA. The electric field can be determined by dividing the applied voltage by the total length of the capillary. Here E has a value of 300 V/cm found by dividing the separation voltage of 15,000 V by a total capillary length of 50 cm. The efficiency of 2,3-DHBA and EOF were evaluated at different PDADMAC concentrations.

**Table 3.3. Efficiency of 2.5 pmol 2,3-DHBA and 0.5% MO at varying concentrations of PDADMAC on a 50  $\mu$ m ID capillary with an applied voltage of 15 kV.**

<b>Coated 50 <math>\mu</math> ID capillary (50 cm length )</b>	<b>Theoretical Plates, N, EOF/MO (0.5%)</b>	<b>Theoretical Plates, N, for 2.5pmol 2,3-DHBA</b>
<b>Uncoated</b>	<b>125,400</b>	<b>67,680</b>
<b>10 mM PDADMAC</b>	<b>79,920</b>	<b>57,720</b>
<b>5 mM PDADMAC</b>	<b>82,260</b>	<b>69,630</b>
<b>1 mM PDADMAC</b>	<b>118,080</b>	<b>103,800</b>
<b>0.5 mM PDADMAC</b>	<b>124,920</b>	<b>105,180</b>

The number of theoretical plates increases with lower concentrations of PDADMAC for 2,3-DHBA which demonstrates that separation is much more efficient for this negatively charged analyte when the EOF is reversed. This allows for sharper peaks and better baseline separation.

#### ***3.4.1.5 Effect of Inner Diameter size on 2,3-DHBA response***

Capillaries of varying inner diameter were used to evaluate detector response for 2.5 pmol 2,3-DHBA to determine optimal separation parameters. Capillaries of 25, 50, and 75  $\mu$ m inner diameter size with a length of 50 cm were utilized.

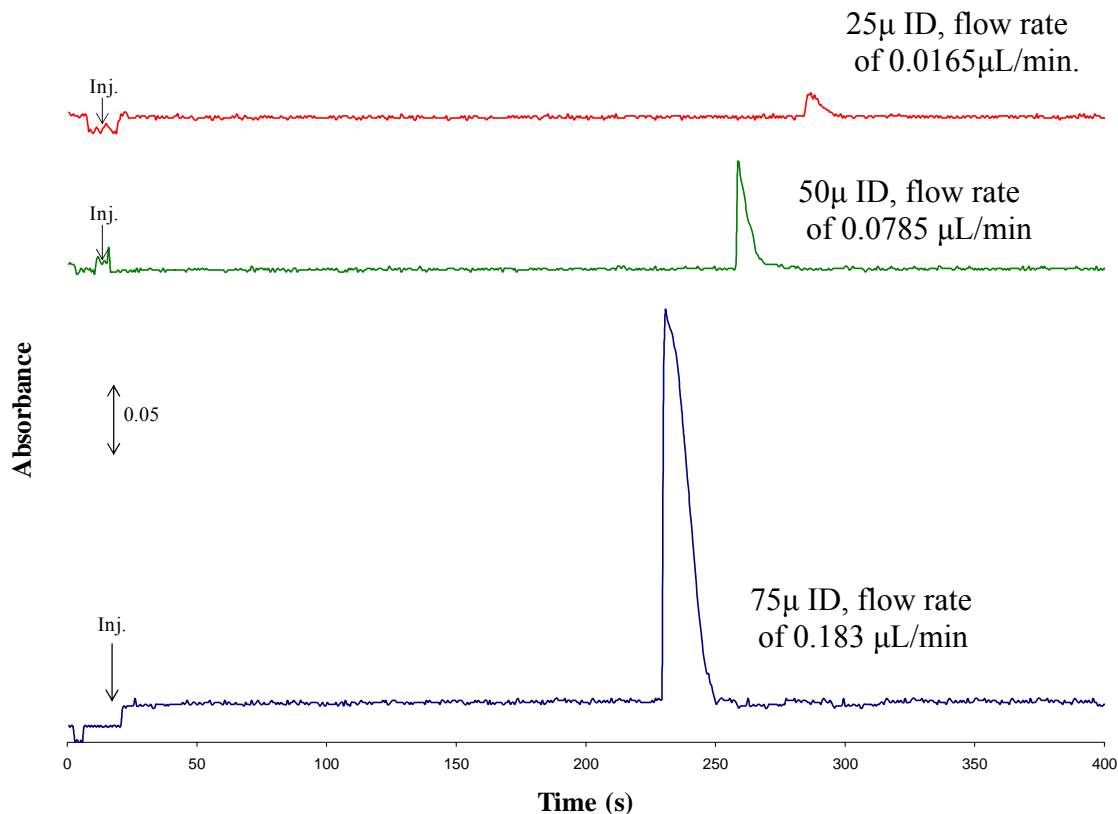


**Figure 21. Electropherograms of 2.5 pmol 2,3-DHBA using 25, 50, 75  $\mu\text{m}$  ID capillaries with an applied voltage of 15 kV.**

This electropherogram shows that UV detector response decreases with capillary inner diameter size. However, this decrease is not directly proportional to capillary ID size. This is because actual transmission of light or pathlength through the capillary is slightly less than the actual capillary inner diameter.<sup>15</sup> Thus the diminishing detector response with decreasing capillary ID will not be a linear trend. Migration times are also slightly lengthened with smaller capillary sizes, because flow becomes more restricted with less volume to migrate through the capillary.

### 3.5 Conclusions

Capillary zone electrophoresis coupled with on-column UV detection is a viable method for quick, efficient separation and detection of the analyte of interest, 2,3-DHBA. This analysis is performed in a discriminating fashion with aqueous conditions mimicking biological pH. Previous CZE separation and detection of 2,3-DHBA has been done at very low pH values or in non aqueous media. By modification of the inner capillary wall with the polycationic electrolyte, PDADMAC, separation was further enhanced by reducing the migration time of 2,3-DHBA from 11 minutes to 3 minutes. A study of the effects of PDADMAC concentration on flow rate, electrophoretic mobility, elution time, and efficiency showed that 1mM PDADMAC provided the optimal coating concentration. This concentration allows for faster migration times, less frequent polymer recoating of the capillary, and high theoretical plate efficiency values that dwarf those found by HPLC. A detection limit study demonstrated the ability to detect concentration values in the 0.3-0.8 pmol range for DA and 2,3-DHBA.

To monitor oxidative stress using 2,3-DHBA, lower concentrations indicative of true conditions in the brain need to be determined (fmol-amol range). While UV detection is widely versatile and fairly discriminating, it lacks the sensitivity needed for these in vivo concentration levels. Electrochemical detection possesses the sensitivity necessary while maintaining the selectivity of UV detection. Using smaller ID capillaries is also advantageous in CZE as the effect of Joule heating is reduced and resulting baselines are more stable. However, as the path length decreases, the detector absorbance response diminishes as well. Fortunately, smaller ID capillaries (< 25  $\mu\text{m}$ ) are favorable for electrochemical detection because they help prevent interference between the applied voltage and detection potential. CZE coupled with UV detection was a good stepping

stone to optimize separation conditions and parameters for 2,3-DHBA. This method illustrated selectivity separating cationic, neutral, and anionic species such as DA, MO, and 2,3-DHBA respectively. The migration time and efficiency of 2,3-DHBA was greatly enhanced by the use of PDADMAC as a capillary coating. These results can be applied to developing electrochemical detection as a useful, sensitive method when coupled with CZE to monitor 2,3-DHBA.

## **Chapter 4: Capillary Zone Electrophoresis Coupled with End-column Electrochemical Detection**

### **4.1 Introduction**

CZE coupled with UV detection provided the optimum separation conditions and parameters for electrochemical determination of 2,3-DHBA. End-column direct and pulsed amperometric detection were performed to improve sensitivity for 2,3-DHBA. This is a novel approach for separating and detecting 2,3-DHBA as there are no previous reports found utilizing CZE/PAD with carbon fiber microelectrodes.

### **4.2 Results and Discussion**

#### ***4.2.1 Oxidation Potential Selection***

The optimal oxidation potential was determined by obtaining cyclic voltammograms (CVs) of each analyte of interest. Choosing a single favorable potential is essential for obtaining high current response and minimal background noise.<sup>49</sup> Selecting a potential beyond each analyte's oxidation peak ensures a reaction at the electrode surface, which in turn generates current measured by the potentiostat. In Figure 22, the CVs of the two main analytes of interest, DA and 2,3-DHBA are shown.

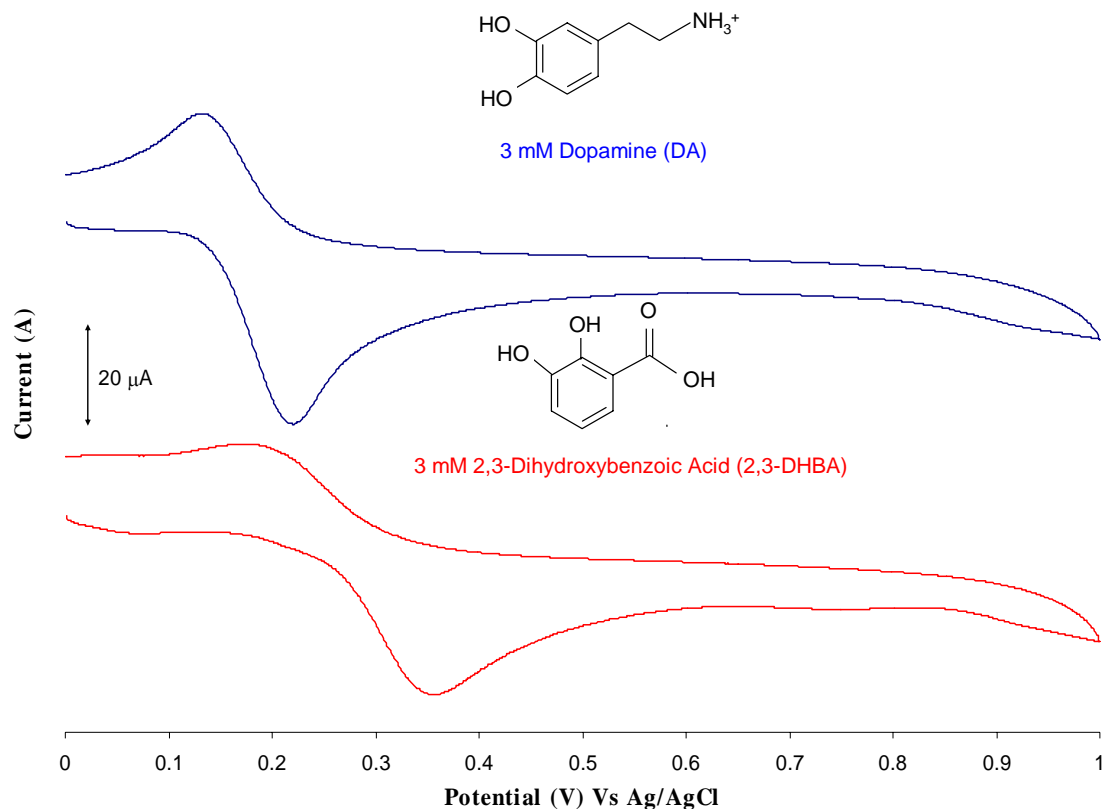


**Figure 22. Cyclic voltammograms of 3 mM DA and 2,3-DHBA in 50mM Phosphate Buffer (pH 7) at 100 mV/s.**

The CV of DA has an oxidation peak at 220 mV, while the CV of 2,3-DHBA yields an oxidation peak at 360 mV vs. Ag/AgCl. An oxidation potential beyond these values should be selected for analyses. An applied potential of 650 mV vs. Ag/AgCl yielded the highest current response for both analytes as it is on the diffusion limited region of the cyclic voltammogram.

#### ***4.2.2 Separation Results with Direct End-Column Amperometric Detection***

The following electropherograms show example separations of DA and catechol (Figure 23), and of DA and 2,3-DHBA (figure 24) respectively. The elution order is



based on the direction of the EOF which is toward the cathodic/detector end of the capillary in both cases. Since the running buffer is at pH 7, DA will be the first to elute (pKa of 8.60), then catechol which acts as an electroactive neutral marker, and lastly 2,3-DHBA (pKa of 2.97). These separations were performed to determine if detection could be achieved electrochemically when coupled with CZE for our system.

Direct amperometry is a simple form of electrochemical detection where the applied potential is held constant and the change in current response is measured as the corresponding signal.

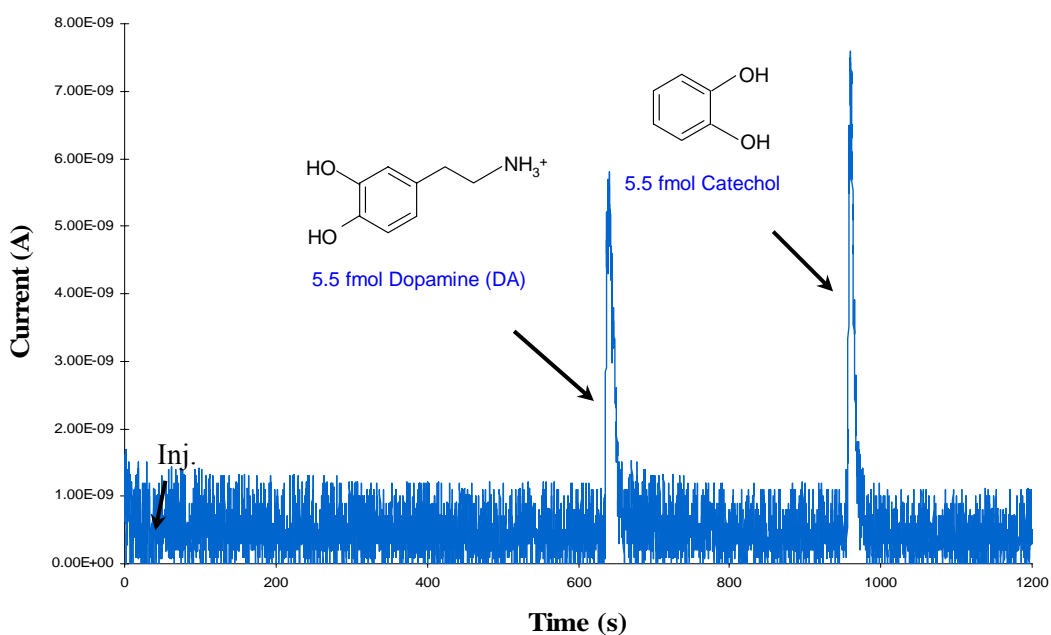


**Figure 23. Electropherogram of 5.5 fmol DA and 5.5 fmol catechol using a 60 cm length 20  $\mu$ m ID capillary with 15kV applied voltage and applied potential of 650 mV.**

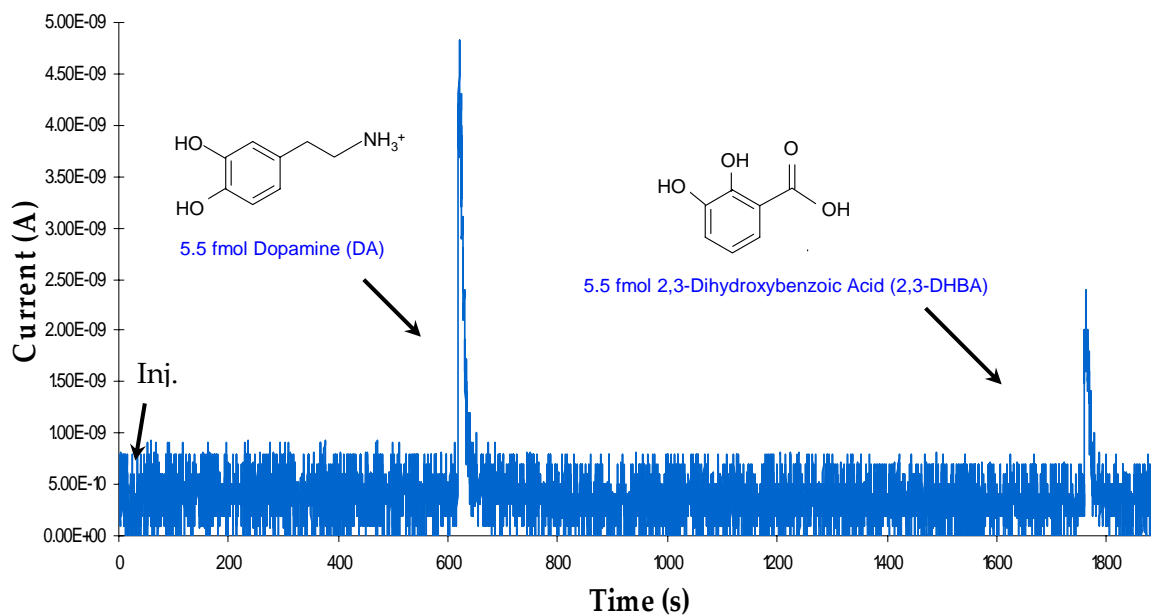


**Figure 24. Electropherogram of 5.5 fmol DA and 5.5 fmol 2,3-DHBA using a 60 cm length 20  $\mu\text{m}$  ID capillary with 15kV applied voltage and applied potential of 650 mV.**

The elution times of DA appear to be approximately about 10 minutes, 15 minutes for catechol, and 30 minutes for 2,3-DHBA. These times are longer than migration times determined with UV detection where detection occurred at a length of 37 cm along the separation capillary. Here, amperometric detection occurs at the end of a 60 cm separation capillary. These electropherograms simply demonstrate that these analytes can be baseline separated by CZE and detected electrochemically. A study was performed to determine the detection limits for DA and 2,3-DHBA with direct amperometric detection.

### 4.2.3 Direct End-Column Amperometry Detection Limits

The following calibration curve and resulting limit of detection (LOD) are for DA.

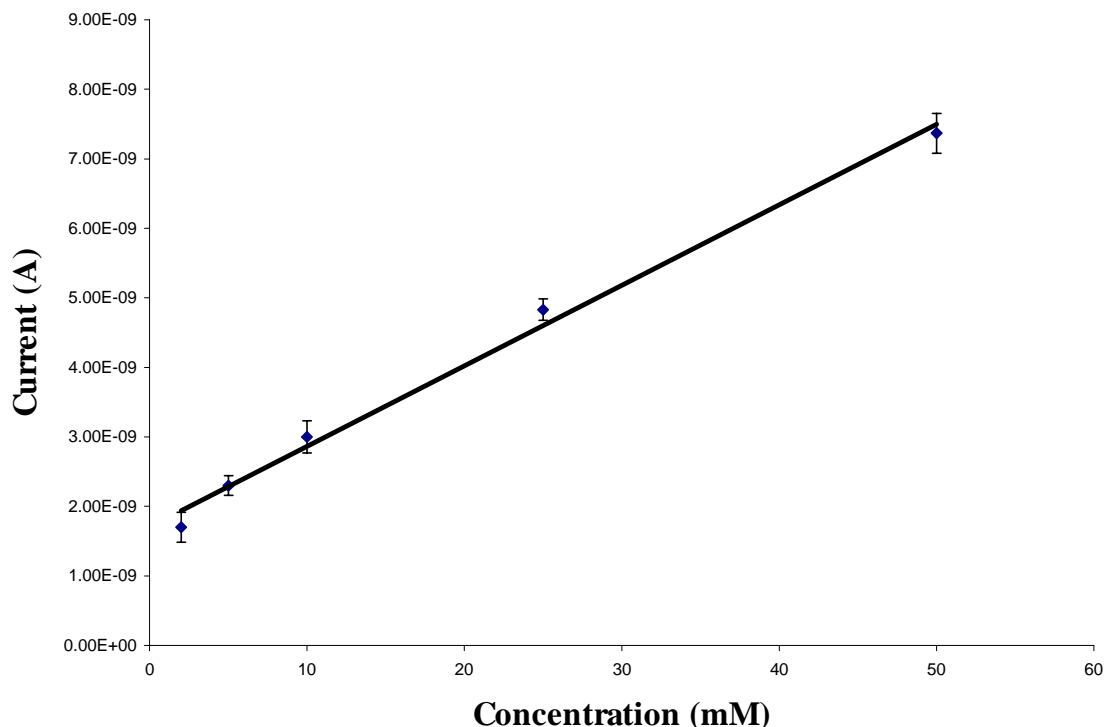


**Figure 25. Calibration curve for DA using a 60 cm length 20 $\mu$ m ID capillary with applied potential of 650mV.**

The amperometric detection limit for DA at 650 mV using a 20  $\mu$ m ID capillary is 0.85 fmol or 0.16 pg. These LODs are 500 times more sensitive than the UV LOD values of 0.49 pmol and 93 pg for a 25  $\mu$ m ID capillary. Reported LOD values for DA determined by CZE/ED utilizing a macro sol-gel carbon working electrode are around 0.30 fmol.<sup>46</sup> The amperometric detection limit for our system is comparable to recent literature values. LOD values are determined by adding the mean background current ( $3.20 \text{ E}^{-10} \text{ A}$ ) to three times the standard deviation of the mean background signal ( $1.48 \text{ E}^{-10}$

<sup>10</sup> A). This sum was divided by the slope of the calibration curve ( $m = 1.00 \text{ E}^{-10}$ ). This gave an LOD in mM which was converted to moles by assuming a volume (of a cone) of  $1.11 \text{ E}^{-10} \text{ cm}^3$  between the end of the capillary and the carbon fiber electrode. The volume of a cone is given as  $\frac{1}{3}\pi r^2 h$  where  $r$  is the radius of the ID of the capillary ( $10 \mu\text{m}$ ) and  $h$  is the height of the exposed carbon fiber which is assumed to be  $10 \mu\text{m}$ . Once the moles of analyte are determined, the mass can be calculated by simply multiplying by the molecular weight of DA ( $189.64 \text{ g/mol}$ ). Again, these LOD values show much improved sensitivity over UV detection for DA. Thus amperometric detection is useful method for monitoring lower concentrations of DA more likely to be found neurologically.

A limit of detection for 2,3-DHBA could not be found because at known concentrations of 20mM and below, the signal-to-noise was too low to distinguish between peaks and baseline. This is a problem associated with amperometric detection for this system since the background noise is fairly high. If the background current could be minimized, the measured faradaic current (analytical signal) would be enhanced. Pulsed amperometric detection (PAD) performs this task, thus allowing analytes namely 2,3-DHBA to be investigated at lower concentrations due to improved signal-to-noise. Essentially by minimizing the background noise, PAD allows for more sensitive detection of DA and 2,3-DHBA.

#### ***4.2.4 Separation Results with End-Column Pulsed Amperometric Detection***

Pulsed amperometric detection (PAD) acts as a single waveform stepping between 0 V and 650 mV with detection occurring near the end of the pulse duration (650

mV). Essentially this means that as solution is flowing out of the end of the capillary, the electrode begins with an applied potential of 0 V. As a pulse potential of 650 mV is applied every 1.25 seconds for this system, any analyte near the electrode tip gets oxidized, in this case DA and 2,3-DHBA. This generates a current response which is measured by the potentiostat. The current response measured at 650 mV is due to faradaic current (our analytical signal) as well as resistive and capacitive current (background noise). As the potential drops back to 0 V, any measured current response is due to resistive and capacitive current and not any oxidized analyte. The current measured at 0 V can then be subtracted from the current response determined at 650 mV. This differential value effectively discriminates the faradaic signal from the capacitive and resistive background currents. This consequently improves signal to noise, allowing for more sensitive detection of 2,3-DHBA.

Separations were conducted to monitor DA and 2,3-DHBA in solution with other ionic species containing dihydroxy groups on aromatic rings. The first electropherogram show the separation of dopamine (DA), 4-aminoresorcinol (4-AR), and catechol. DA and 4-AR are cationic species so no capillary modification with PDADMAC is necessary for fast elution times. The peak oxidation potentials of 4-AR and catechol in phosphate buffer (pH 7) are 440 mV and 300 mV respectively. These were determined by CV as described in section 3.2.1. Thus an applied pulse potential of 650 mV is acceptable for analysis of all three compounds.

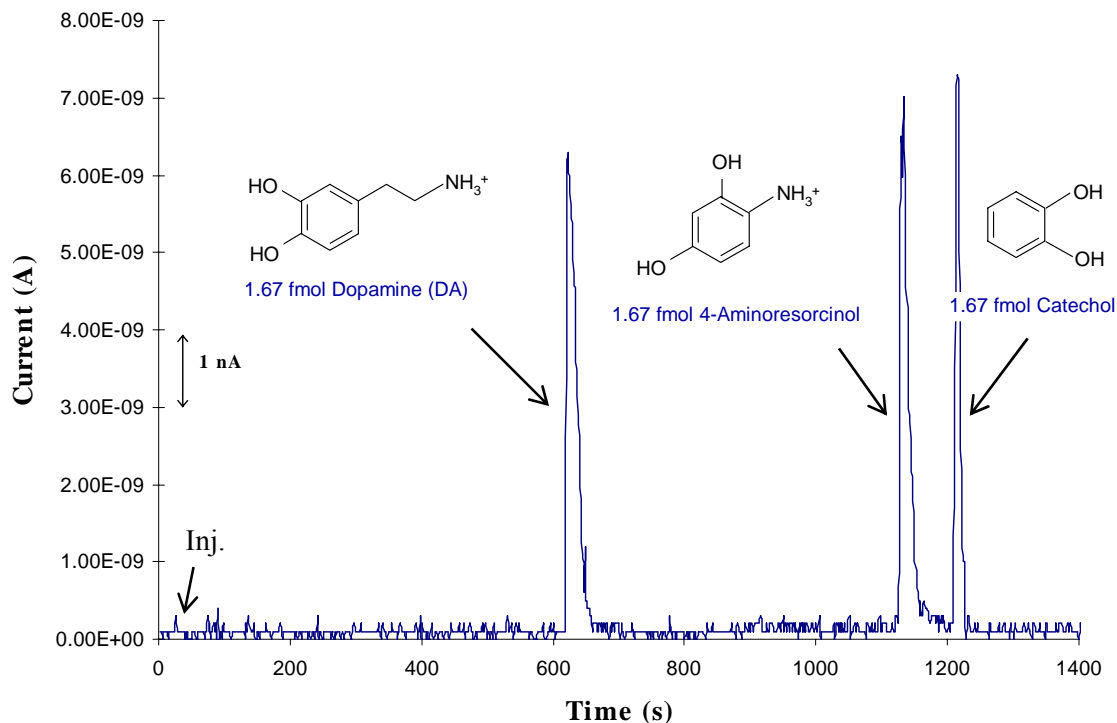


**Figure 26. Pulsed electropherogram of 1.67 fmol DA, 4-AR, and Catechol using a 60 cm length 20  $\mu$ m ID capillary with separation voltage of 15 kV.**

Elution times appear to be approximately 10 minutes for DA, 18.5 minutes for 4-AR, and 20 minutes for catechol. Separation and detection of these compounds with CZE/PAD was also successfully performed at quantities of 3.33 and 0.555 fmol. The background noise seems to be greatly reduced, and the peaks appear more well-defined. With direct amperometric detection, baseline separation of 4-AR and catechol is not as easily achieved.

The second electropherogram illustrates the separation of 2,3-DHBA and DOPAC, which is a metabolite of dopamine. These species are both anionic at pH 7 with pKa values of 2.97 (2,3-DHBA) and  $\sim$ 4.5 (DOPAC). Capillary modification with PDADMAC is necessary for time-efficient separation. This procedure is described in

section 3.1.4. The oxidation potential of DOPAC determined by CV was 505 mV, so the pulse potential of 650 mV is again viable for both compounds. Salicylic acid (SA) and ascorbic acid (AA) were also investigated as possible anionic species for separation. However, SA has an oxidation potential of 1.07 V which is past the limit for 2,3-DHBA, and AA coelutes with DOPAC as it has a similar pKa (4.10).

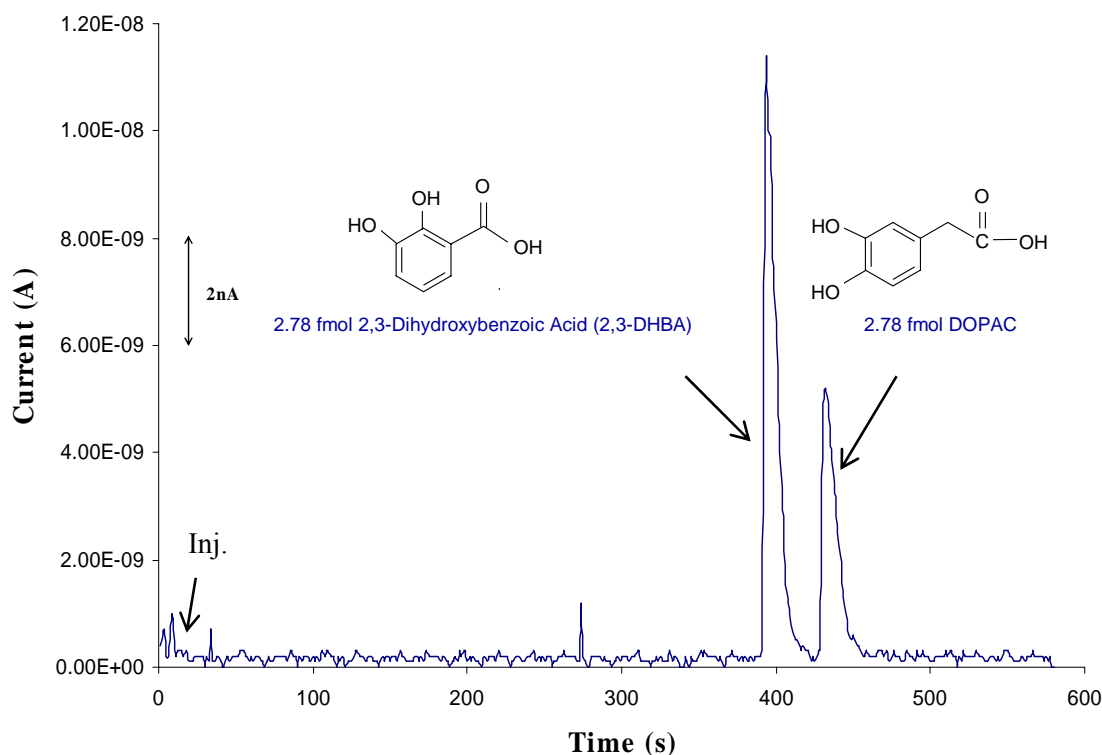


**Figure 27. Pulsed electropherogram of 2.78 fmol 2,3-DHBA and DOPAC using a 60 cm length 20  $\mu$ m ID capillary with separation voltage of 15 kV.**

Elution times are 6.5 minutes for 2,3-DHBA and 7.0 minutes for DOPAC. This is an excellent example of how well PAD allows for baseline separation through reduced background noise. These two compounds which elute extremely close to one another are

clearly two distinct, resolved peaks. Separation and detection with CZE/PAD was also achieved for these compounds at levels of 1.1, 0.55, and 0.22 fmol. All electropherograms are to illustrate that separation and detection can be performed for DA and 2,3-DHBA at varying concentrations in solution with other charged species. The separation data suggests that PAD is a useful detection method for CZE by improving sensitivity and baseline stability by minimizing noise that could dwarf the measured current response signal.

#### 4.2.5 Pulsed Amperometric Limits of Detection

Limits of detection for both DA and 2,3-DHBA were determined using CZE/PAD using the following calibration curves.

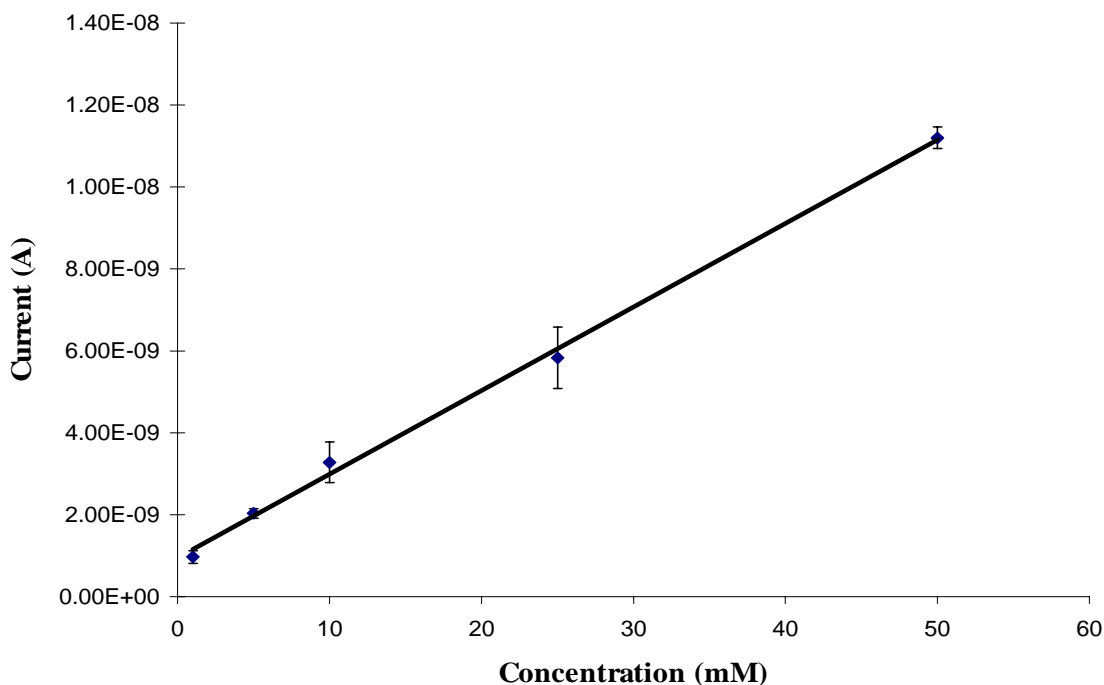


**Figure 28. Calibration curve for DA using a 60 cm length 20  $\mu$ m ID capillary with a pulsed potential of 650mV.**



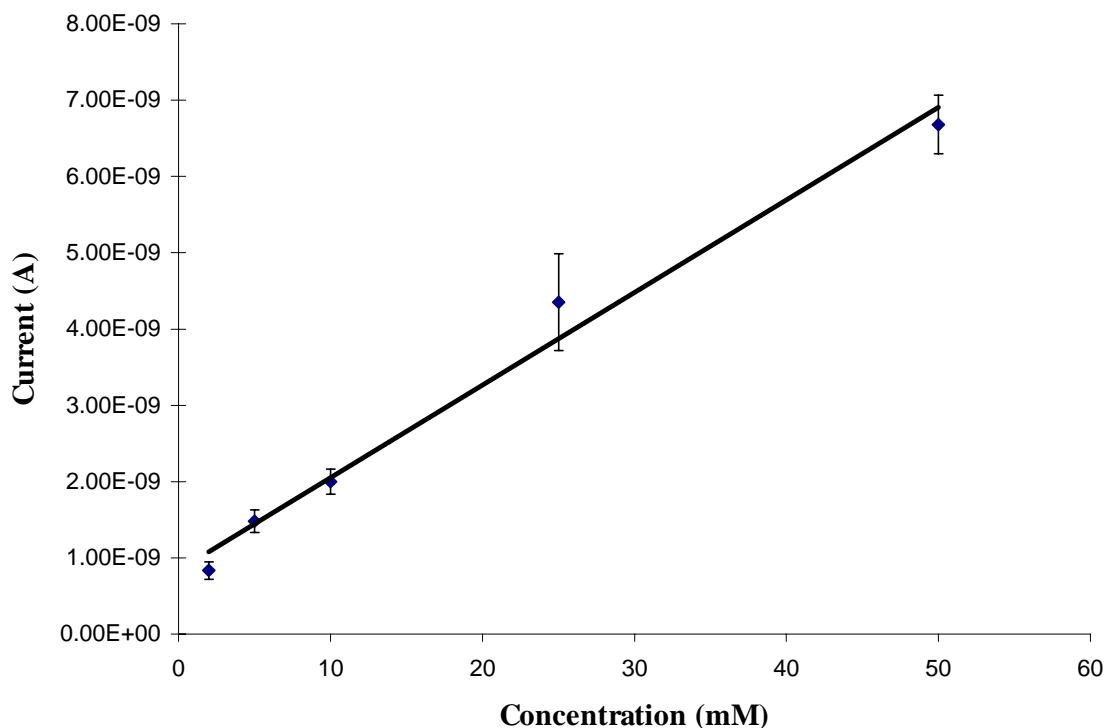


**Figure 29. Calibration curve for 2,3-DHBA using a 60 cm length 20  $\mu\text{m}$  ID capillary with a pulsed potential of 650 mV.**

The pulsed amperometric LOD for DA is 0.44 fmol or 84 fg. These values were calculated the by same way described in section 3.2.3. The slope for this curve was  $2.00 \text{ E}^{-10}$  with a mean background signal of  $3.4 \text{ E}^{-10} \text{ A}$  and a standard deviation of  $1.52 \text{ E}^{-10} \text{ A}$ . These LODs are very similar to the values determined for direct amperometric detection.

The PAD limit of detection for 2,3-DHBA is 1.0 fmol or 0.16 pg. These concentration and mass values were determined using a slope of  $1.00 \text{ E}^{-10}$  from the curve in Fig. 9, a mean background/blank signal as  $2.60 \text{ E}^{-10} \text{ A}$ , and its standard deviation of  $2.19 \text{ E}^{-10} \text{ A}$ . These LOD values are far more sensitive than UV LODs for 2,3-DHBA of 0.53 pmol or 81 pg using a 25  $\mu\text{m}$  ID capillary. Again, LOL could not be determined as concentrations exceeding 50 mM were not evaluated.

### 4.3 Conclusions

Capillary zone electrophoresis coupled with end-column amperometric detection was successfully developed as a useful, working system for the separation of DA and namely 2,3-DHBA from other catechol species. DA and 2,3-DHBA can be separated and monitored with greater sensitivity using amperometric detection in aqueous media at biological pH. A detection limit study showed that DA could be determined in the 0.849 fmol range as compared to 0.2-0.4 pmol for UV detection. Unfortunately, background contributions from capacitive and resistive current was too high to investigate 2,3-DHBA at concentration levels below 2.2 fmol or 0.34 pg, so an LOD study could not be performed. Pulsed amperometric detection was then employed as a technique so 2,3-DHBA could be monitored at lower concentrations.

PAD minimizes the background noise, so the measured current response is mostly due to the reaction at the electrode. Separations with well-defined peaks and smooth, stable baselines were achieved with cationic species (DA, 4-AR, and neutral Catechol) and anionic species (2,3-DHBA and DOPAC) at pH 7. The analysis of the anionic species was further enhanced by modification of the capillary with the cationic polymer PDADMAC. Reversal of the EOF allowed 2,3-DHBA to elute much more quickly (6.5 minutes) than it did on an unmodified capillary (30 minutes). These separations are fairly novel, as most studies concerning CZE/PAD utilize gold or platinum microelectrodes instead of carbon fibers. There have been a few studies performed with HPLC coupled with PAD using carbon fiber microelectrodes, but none investigate neurotransmitters, catechols, or 2,3-DHBA as an oxidative stress marker. A limit of detection study illustrated the sensitivity of PAD with concentration values of 0.44 fmol/ 84 fg for DA

and 1.0 fmol/ 16 fg for 2,3-DHBA. These concentration levels are applicable to monitoring oxidative stress conditions in the brain. Previous studies using HPLC-ED have determined in vivo detection of 2,3-DHBA at 0.37 nmol<sup>11</sup> and 3.0-3.5 pg<sup>47</sup>. Recent studies determined levels of 0.024 fmol or 3.6 fg for 2,3-DHBA using CZE with amperometric detection with a macro carbon disk electrode.<sup>10</sup> PAD rivals this sensitivity and could surpass these values with development of precise electrode placement. This could be achieved with the use of a scanning electrochemical microscope, currently under development and optimization in our lab now.

CZE coupled with amperometric detection has proved a very practical method for the separation and detection of 2,3-DHBA and other compounds of interest like DA. PAD especially demonstrates the sensitivity and versatility needed for monitoring our analytes of interest which are all electroactive. The studies performed with UV detection yielded the optimum separation conditions for 2,3-DHBA such as separation voltage and PDADMAC concentration. While UV detection offers selectivity for ionic and neutral species of interest, CZE/PAD is a more suitable technique for the analysis of 2,3-DHBA as a marker for neurological oxidative stress.

## **Chapter 5: Summary and Future Work**

### **5.1 Summary**

Oxidative stress is postulated to contribute to the onset of Parkinson's Disease by generation of the highly toxic and reactive hydroxyl radical. The  $\bullet\text{OH}$  radical can attack neuron cells, leading to cell degeneration and death. The reactivity of the  $\bullet\text{OH}$  radical makes it difficult to monitor, so it must be trapped with salicylic acid to measure its production. The main, non-enzymatic product of trapping  $\bullet\text{OH}$  with salicylic acid is 2,3-dihydroxybenzoic acid. This compound is used as a marker for oxidative stress. When this trapping mechanism is applied to humans and animals, sample sizes are limited to  $\mu\text{L}$  volumes. Capillary zone electrophoresis requires minimal sample volume, so this elution technique is a viable analysis method. Here, rapid and efficient separation conditions such as separation voltage and electroosmotic flow control were found for determination of 2,3-DHBA by coupling CZE with ultraviolet detection, a versatile, detection scheme in CE. These optimal separation conditions were then applied to determining 2,3-DHBA electrochemically. Using CZE coupled with pulsed amperometric detection, sensitivity was heightened for lower detection limits of 2,3-DHBA. This is a novel and practical approach for separating and detecting 2,3-DHBA. This method would be useful in monitoring 2,3-DHBA as a marker for oxidative stress.

### **5.2 Future Work**

Higher sensitivity for 2,3-DHBA could be achieved with exact, reproducible electrode placement at the end of the capillary. Exact electrode placement becomes possible with the use of a scanning electrochemical microscope (SECM). The SECM

scans a square area over the end of the capillary, with a working carbon fiber microelectrode. The current response is recorded as an electroactive species continually flows out the end of the capillary. After the scan is complete, a topographical map is generated which shows the area of highest current response indicating the end of the capillary. With the electrode placed at this particular spot each time, signal to noise will be highest resulting in better sensitivity for 2,3-DHBA determination. The SECM is currently under development in our lab.

Another future application is coupling CZE/PAD with microdialysis for direct in-line monitoring of oxidative stress *in vivo*. The small sample volumes and flow rates in microdialysis are synonymous with the small volumes utilized in CZE. If oxidative stress conditions were induced, dialysate from the brain could then react with salicylic acid. The presence of 2,3-DHBA would be indicative of the oxidative stress  $\bullet\text{OH}$  formation.

Rapid and sensitive determination of 2,3-DHBA with CZE/PAD has many possible neurological applications. CZE/PAD is an exciting, novel method for the separation and detection of 2,3-DHBA as a marker for oxidative stress.

## References

- (1) National Parkinson Foundation [www.parkinson.org](http://www.parkinson.org)
- (2) Obata, T. *Toxicology Letters* **2002**, *132*, 83-93.
- (3) Garris, P.A.; Wightman, R.M. *Synapse* **1995**, *20*, 269-279.
- (4) Ebadi, M.; Srinivasan, S.K.; Baxi, M.D. *Progress in Neurobiology* **1996**, *48*, 1-19.
- (5) Jacobsson, S.O.P.; Fowler, C.J. *Neurochem. Int.* **1999**, *34*, 49-62.
- (6) Loikkanen, J.J.; Naarala, J.; Savolainen, K.M.; *Free Rad. Bio. Med.* **1998**, *24(2)*, 377-384.
- (7) Yang, C.; Tsai P.; Lin, N.; Liu, L.; Kuo, J. *Free Rad. Bio. Med.* **1995**, *19(4)*, 453-459.
- (8) Blandini, F.; Martigoni, E.; Ricotti, R.; di Jeso, F.; Nappi, G. *J. Chromatogr. B* **1999**, *732*, 213-220.
- (9) Ghiselli, A.; Laurenti, O.; De Mattia, G.; Maiani, G.; Ferro-Luzzi, A. *Free Rad. Bio. Med.* **1992**, *13*, 621-626.
- (10) Wang, Q.; Ding, F.; Zhu, N.; Li, H.; He, P.; Fang, Y. *J. Chromatogr. A* **2003**, *1016*, 123-128.
- (11) Coudray, C.; Favier, A. *Free Rad. Bio. Med.* **2000**, *29(11)*, 1064-1070.
- (12) Tabatabaei, A.; Abbott, F.S. *Free Rad. Bio. Med.* **1999**, *26(7-8)*, 1054-1058.
- (13) Kumarathasan, P.; Vincent, R.; Goegan, P.; Potvin, M.; Guenette, J. *Biochem. Cell. Biol.* **2001**, *79*, 33-42.
- (14) Jorgenson, J.W.; Lukacs, K.D. *Anal. Chem.* **1981**, *53*, 1298-1302.
- (15) Landers, J. *Handbook of Capillary Electrophoresis*; 2<sup>nd</sup> ed.; CRC Press: New York, 1997.
- (16) Jorgenson, J.W.; Lukacs, K.D. *Clin. Chem.* **1981**, *27(9)*, 1551-1553.
- (17) Weinberger, R. *Practical Capillary Electrophoresis*, Academic Press, Inc.: New

York, 1993.

(18) Jorgenson, J.W.; Lukacs, K.D. *Science* **1983**, 222, 266-272.

(19) Altria, K.D. *Capillary Electrophoresis Guidebook: Methods in Molecular Biology*; vol. 52; Humana Press: Totowa, NJ, 1996.

(20) Kennedy, R.T.; Oates, M.D.; Cooper, B.R.; Nickerson, B.; Jorgenson, J.W. *Science* **1989**, 246, 57-63.

(21) Chen, M.; Huang, H. *Anal. Chem.* **1995**, 67, 4010-4014.

(22) Tsuda, T.; Nomura, K.; Nakagawa, G. *J. Chromatogr.* **1983**, 264, 385-392.

(23) Walbroehl, R.; Jorgenson, J.W. *J. Chromatogr.* **1984**, 315, 135-143.

(24) Tjornelund, J.; Bazzanella, A.; Lochmann, H.; Bachmann, K. *J. Chromatogr. A* **1998**, 811, 211-217.

(25) Coolen, S.A.J.; Huf, F.A.; Reijenga, J.C. *J. Chromatogr. B* **1998**, 717, 119-124.

(26) Wallingford, R.A.; Ewing, A.G. *Anal. Chem.* **1987**, 59, 1762-1766.

(27) McNally, M.; Wong, D.K.Y. *Anal. Chem.* **2001**, 73, 4793-4800.

(28) Buchberger, W.W. *J. Chromatogr. A* **2000**, 884, 3-22.

(29) Holland, L.A.; Lunte, S.M. *Anal. Comm.* **1998**, 35, 1H-4H.

(30) Logman, M.J.; Budygin, E.A.; Gainetdinov, R.R.; Wightman, R.M. *J. Neurosci. Meth.* **2000**, 95, 95-102.

(31) Wallingford, R.A.; Ewing, A.G. *Anal. Chem.* **1988**, 60, 1972-1975.

(32) Wallingford, R.A.; Ewing, A.G. *Anal. Chem.*, **1988**, 60, 258-263.

(33) Everett, W.R.; Bohs, C.; Davies, M. *Curr. Sep.* **2000**, 19(1), 25-28.

(34) Goto, M.; Inagaki, S.; Esaka, Y. *Anal. Sci.*, **2001** 17, 1383-1387.

(35) Chen, G.; Ye, J.N.; Cheng, J.S. *Chromatographia* **2000**, 52 (3-4), 137-141.

- (36) Osbourn, D.M.; Lunte, C.E. *Anal. Chem.* **2001**, *73*, 5961-5964.
- (37) Jin, W.; Jin, L.; Shi, G.; Ye, J. *Anal. Chim. Acta* **1999**, *382*, 33-37.
- (38) Li, H.; Wang, Q. *Anal. Bioanal. Chem.* **2004**, *378*, 1801-1805.
- (39) Kuhn, R.; Hoffstetter-Kuhn, S. *Capillary Electrophoresis: Principles and Practice*; Springer-Verlag: New York, 1993.
- (40) Siren, H.; Mielonen, M.; Herlevi, M. *J. Chromatogr. A* **2004**, *1032(1-2)*, 289-297.
- (41) Vuorensola, K.; Siren, H.; Kostiainen, R.; Kotiaho, R. *J. Chromatogr. A* **2002**, *979(1-2)*, 179-189.
- (42) Melanson, J.E.; Baryla, N.E.; Lucy, C.A. *Trends Anal. Chem.* **2001**, *20(6-7)*, 365-374.
- (43) Fritz, J.S.; Breadmore, M.C.; Hilder, E.F.; Haddad, P.R. *J. Chromatogr. A* **2002**, *942*, 11-32.
- (44) Cohen, N.; Grushka, E. *J. Cap. Elec.* **1994**, *1(2)*, 112-115.
- (45) Liu, Q.; Lin, F.; Hartwick, R.A. *J. Chromatogr. Sci.* **1997**, *36*, 126-130.
- (46) Hua, L.; Tan, S.N. *Anal. Chim. Acta* **2000**, *403(1-2)*, 179-186.
- (47) Patthy, M.; Kiraly, I.; Sziraki, I. *J. Chromatogr. B* **1995**, *664*, 247-252.
- (48) Heinze, J. *Agnew. Chem. Int. Ed. Eng.* **1993**, *32*, 1268-1288.
- (49) Coudray, C.; Talla, M.; Martin, S.; Fatome, M.; Favier, A. *Anal. Biochem.* **1995**, *227*, 101-111.
- (50) O'Shea, T.J.; Lunte, S.M. *Curr. Sep.* **1995**, *14(1)*, 18-23.
- (51) Cao, Y.; Chu, Q.; Ye, J. *Anal. Bioanal. Chem.* **2003**, *376*, 691-695.
- (52) Robert, F.; Bert, L.; Denoroy, L.; Renaud, B. *Anal. Chem.* **1995**, *67*, 1838-1844.
- (53) Zhou, S.Y.; Zuo, H.; Stobaugh, J.F.; Lunte, C.E.; Lunte, S.M. *Anal. Chem.* **1995**,



67, 594-599.

(54) Kim, W.-S.; Dahlgren, R.L.; Moroz, L.L.; Sweedler, J.V. *Anal Chem.* **2002**, *74*, 5614-5620.

(55) Blatny, P.; Kvasnicka, F.; Kenndler, E. *J. Chromatogr. A* **1997**, *757*, 297-302.

(56) Martinez, D.; Pocurull, E.; Marce, R.M.; Borrull, F.; Calull, M. *J. Chromatogr. A* **1996**, *734*, 367-373.

(57) Sloss, S.; Ewing, A. *Anal. Chem.* **1993**, *63*, 577-581.

(58) Wallenberg, S.R.; Nyholm, L., Lunte, C.E. *Anal. Chem.* **1999**, *71*, 544-549.

(59) O'Shea, T.J.; Lunte, S.M. *Anal. Chem.* **1993**, *65*, 948-951.

(60) LaCourse, W.R.; Owens, G.S. *Electrophoresis* **1996**, *17*, 310-318.

(61) LaCourse, W.R.; Owens, G.S. *J. Chromatogr. B* **1997**, *695*, 15-25.

(62) Guzman, A.; Augi, L.; Pedrero, M.; Yanez-Sedeno, P.; Pingarron, J.M. *J. Pharm. Biomed. Anal.* **2003**, *33*, 923-933.

## **Vita**

Stephanie E. Hooper was born in Greenville, SC on September 13, 1978 to Iris and William Hooper. She has a sister Emily four years her junior. Her family then lived outside Atlanta, GA until she was ten. She and her family then moved to Mt. Pleasant, SC across the river from Charleston, SC where she attended and graduated from Wando High School. She then pursued a Bachelor's of Science in chemistry at the University of South Carolina, where she graduated in May 2000. She worked for a year as an environmental chemist at Shealy Environmental Services, Inc. in Cayce, SC. She then decided to further her education by pursuing a graduate degree in analytical chemistry at Virginia Tech. She did research under the advisement of Dr. Mark R. Anderson, and she completed her Master's of Science in August of 2004. She plans to return to Charleston, SC for the time-being to be with her family while working at High Purity Standards as an analytical chemist. Beyond that, the sky's the limit.